



Western Washington University
Western CEDAR

WWU Graduate School Collection

WWU Graduate and Undergraduate Scholarship

Spring 1990

Tidal-flushing Characteristics of the Proposed Lummi Bay Marina, Whatcom County, Washington

William Morse Watts

Western Washington University, wmsbwatts@aol.com

Follow this and additional works at: <https://cedar.wwu.edu/wwuet>



Part of the [Geology Commons](#)

Recommended Citation

Watts, William Morse, "Tidal-flushing Characteristics of the Proposed Lummi Bay Marina, Whatcom County, Washington" (1990). *WWU Graduate School Collection*. 720.

<https://cedar.wwu.edu/wwuet/720>

This Masters Thesis is brought to you for free and open access by the WWU Graduate and Undergraduate Scholarship at Western CEDAR. It has been accepted for inclusion in WWU Graduate School Collection by an authorized administrator of Western CEDAR. For more information, please contact westerncedar@wwu.edu.

TIDAL-FLUSHING CHARACTERISTICS OF THE
PROPOSED LUMMI BAY MARINA,
WHATCOM COUNTY, WASHINGTON

by

William Morse Watts

accepted in partial completion
of the requirements for the degree of
Master of Science

~~_____~~
Dean of the Graduate School

Advisory Committee

~~_____~~
Chair

~~_____~~
~~_____~~

MASTER OF SCIENCE THESIS

In presenting this thesis in partial fulfillment of the requirements for a master's degree at Western Washington University, I agree that the Library shall make its copies freely available for inspection. I further agree that extensive copying of this thesis is allowable only for scholarly purposes. It is understood, however, that any copying or publication of this thesis for commercial purposes, or for financial gain, shall not be allowed without my written permission.

Signature _____

Date 6/13/90

MASTER'S THESIS

In presenting this thesis in partial fulfillment of the requirements for a master's degree at Western Washington University, I grant to Western Washington University the non-exclusive royalty-free right to archive, reproduce, distribute, and display the thesis in any and all forms, including electronic format, via any digital library mechanisms maintained by WWU.

I represent and warrant this is my original work, and does not infringe or violate any rights of others. I warrant that I have obtained written permissions from the owner of any third party copyrighted material included in these files.

I acknowledge that I retain ownership rights to the copyright of this work, including but not limited to the right to use all or part of this work in future works, such as articles or books.

Library users are granted permission for individual, research and non-commercial reproduction of this work for educational purposes only. Any further digital posting of this document requires specific permission from the author.

Any copying or publication of this thesis for commercial purposes, or for financial gain, is not allowed without my written permission.

William M. Watts
February 23, 2018

TIDAL-FLUSHING CHARACTERISTICS OF THE
PROPOSED LUMMI BAY MARINA,
WHATCOM COUNTY, WASHINGTON

A thesis presented to the Faculty
of Western Washington University

in partial fulfillment
of the requirement for the degree of
Master of Science

by

William Morse Watts

June, 1990

ABSTRACT

Tidal-flushing of the proposed Lummi Bay Marina was studied using a physical model. The model was distinct from those of other regional marinas in that it included a berm around the edges, depth contours, sloping walls, and simulated mixed-semidiurnal tides. Spectrophotometric measurements of absorbance of dye in water resulted in the calculation of exchange-coefficients and flushing efficiency. Exchange coefficients in the physical model increased with increasing tidal range, suggesting a tendency for decreased water quality during smaller tides. Exchange was best in spring-tide simulations, but water tended to stagnate during the smaller ebb and flood cycles in both spring and neap simulations. Water quality in the proposed Lummi Bay Marina will probably also vary with tidal range and may be vulnerable to depletion of dissolved oxygen and increased temperature during periods of smaller tidal exchange.

Circulation gyres forming in the model contained less-mixed water toward their centers than at their edges. The primary counterclockwise-gyre retained enough momentum to remain intact throughout a tidal cycle. Neap tides did not induce as strong a circulation of water as did spring tides. Secondary clockwise-gyres formed in the north and south corners of the model over the berm. Those gyres were destroyed each time the berm was exposed, causing short-term water-quality problems. In the event of construction of the marina, the problem of tidal-flushing should be studied using a field approach to verify the results of this study.

ACKNOWLEDGEMENTS

This project would not have been possible without the help of a number of people. I wish to thank my committee members, Dr. Maury Schwartz, Dr. Chris Suczek, and Dr. Tom Terich, for their comments and criticisms of my work. I also thank George Mustoe for the hours of brainstorming and footwork that made possible the innovations used in the project. Without him it would have been impossible to proceed. Dave Schuldt and Norm Skjelbreia of the U. S. Army Corp of Engineers kindly provided much of the information used here. The Lummi Tribe provided access to the aquaculture pond. Dr. Ronald Nece of the UW Department of Civil Engineering was very helpful in getting me pointed in the right direction. Clinton Burgess of the WWU Instrument Center showed me proper laboratory methods. Russ Karns photographed the aquaculture pond from the air. Dr. Richard Fonda, WWU Department of Biology, reviewed my statistics.

I would also like to thank the faculty, staff, and students of WWU's Department of Geology who made my stay here worthwhile. Finally, thanks go to Sarah and my parents, all of whom not only encouraged and supported me, but also put up with me.

TABLE OF CONTENTS

Abstract	i
Acknowledgements	ii
List of Figures	v
List of Tables	vii
Introduction	1
Statement of Problem	10
Related Investigations	18
Methods	21
Scale Models	21
Design of the Model	23
Model Construction	25
Design and Construction of the Tide Generator	25
Calibration Procedures	27
Calibration of Timing	27
Calibration of Height	31
Dye Selection and Calibration	32
Quantitative Methods	35
Qualitative Methods	39
Results	40
Flushing Coefficients	40
Spring-tide Trial Runs	40
Neap-tide Trial Runs	47
Discussion	49
Tidal Exchange	49

Effects of the Berm on Circulation	50
Effects of Sloping Dikes and Berm-walls on Circulation	51
Effects of Non-uniform Bottom Depth	52
Effects of a Simulated Diurnal Inequality	52
Conclusions	54
References Cited	56

LIST OF FIGURES

Figure 1	Location map of proposed Lummi Bay Marina and five other marinas to which it was compared	2
Figure 2	Map of Lummi Bay showing Lummi Sea Pond aquaculture site	3
Figure 3	Oblique aerial view of Lummi Bay to west showing aquaculture pond and Sandy Point. River channel is roughly where the access channel to the proposed marina would lie	6
Figure 4	Composite oblique aerial view of Lummi Bay and surrounding landforms. Proposed marina site is situated in the aquaculture pond where photos overlap. Note drainage of Lummi River across the tidal flat. Sandy Point is at far left (photos by Russ Karns)	7
Figure 5	Plan of proposed Lummi Bay Marina showing terminology used in this study. Depths and berm widths are labeled. Datum for depths is Mean Lower Low Water (MLLW)	11
Figure 6	Neap-tide curve used for physical-model simulation of tides at Lummi Bay. Units are expressed in terms of the prototype	26
Figure 7	Spring-tide curve used for physical-model simulation of tides at Lummi Bay. Units are expressed in terms of the prototype	27
Figure 8	Photograph of the Lummi Bay Marina physical model	28
Figure 9	Photograph of the tide-generator used in this study	29
Figure 10	Photograph of the tide-generator from another angle showing motor, transmission system, cams, and cam-follower	30
Figure 11	Wavelength vs absorbance of Mrs. Stewart's Laundry Bluing as detected by the IBM double-beam spectrophotometer showing strong light-absorbance by bluing at the 680 nm wavelength. Note that the curve of the tap-water blank solution is also plotted	33
Figure 12	Plot of bluing concentration vs absorbance. The linear relationship indicates that bluing	

	absorbs light as predicted by Beer's Law	35
Figure 13	Mean local exchange-coefficients for sample locations from 10 spring-tide trial runs. Each trial run simulated two lunar days (four tidal cycles). Water was sampled at LLW. Mean exchange for spring-tides was $E_{av} = 0.50$	41
Figure 14	Mean local exchange-coefficients for sample locations from 10 neap-tides trial runs. Each trial run simulated two lunar days (four tidal cycles). Water was sampled at LLW. Mean exchange for neap-tides was $E_{av} = 0.22$	42
Figure 15	Exchange coefficient vs tidal range for physical-model tests of six Pacific Northwest marinas	43
Figure 16	Tidal prism ratios vs tidal range for physical-model tests of six Pacific Northwest marinas	44
Figure 17	Flushing efficiency vs tidal range for physical-model tests of six Pacific Northwest marinas	45

LIST OF TABLES

Table 1	Conversion factors: U.S. customary to metric (SI) units of measurement	5
Table 2	Relationships of scaled dimensions between model and prototype of the Lummi Bay Marina	22
Table 3	Tidal heights used in the physical model of the proposed Lummi Bay Marina	36

INTRODUCTION

The U.S. Army Corps of Engineers (1988) has proposed the construction of a 435-berth marina within an existing diked aquaculture pond located in Lummi Bay. The project has been designed to shelter small fishing-craft which are used for salmon fishing in the Strait of Georgia. Water quality in marinas in the Pacific Northwest is important because they serve as habitat for a variety of species of fish, while simultaneously they are potential sources of pollution. The present study was undertaken to determine whether the proposed marina will be adequately flushed through tidal action.

Lummi Bay is a large shallow estuary located in western Whatcom County, Washington. The bay, about 6 square miles in extent, is connected to the southern Strait of Georgia to the west and is contained on the north and east by the mainland. The southern exposure is protected by Lummi Island (Figures 1 and 2). Historically, the Nooksack River drained alternately into both Lummi Bay and Bellingham Bay, but around 1860 the river was blocked by a log jam that caused it to drain into Bellingham Bay (Easterbrook, 1973). In the intervening years, the river was diked and channelized to flow into Bellingham Bay, the Lummi Bay channel system being used only during periods of flood discharge. The remnants of the Nooksack's Lummi Bay distributary system are called the Lummi or Red River. The 5-mile-long river channel currently drains only a few square miles of farmland and wooded upland, with most of the water moving through a system of drainage ditches before being pumped into the river.

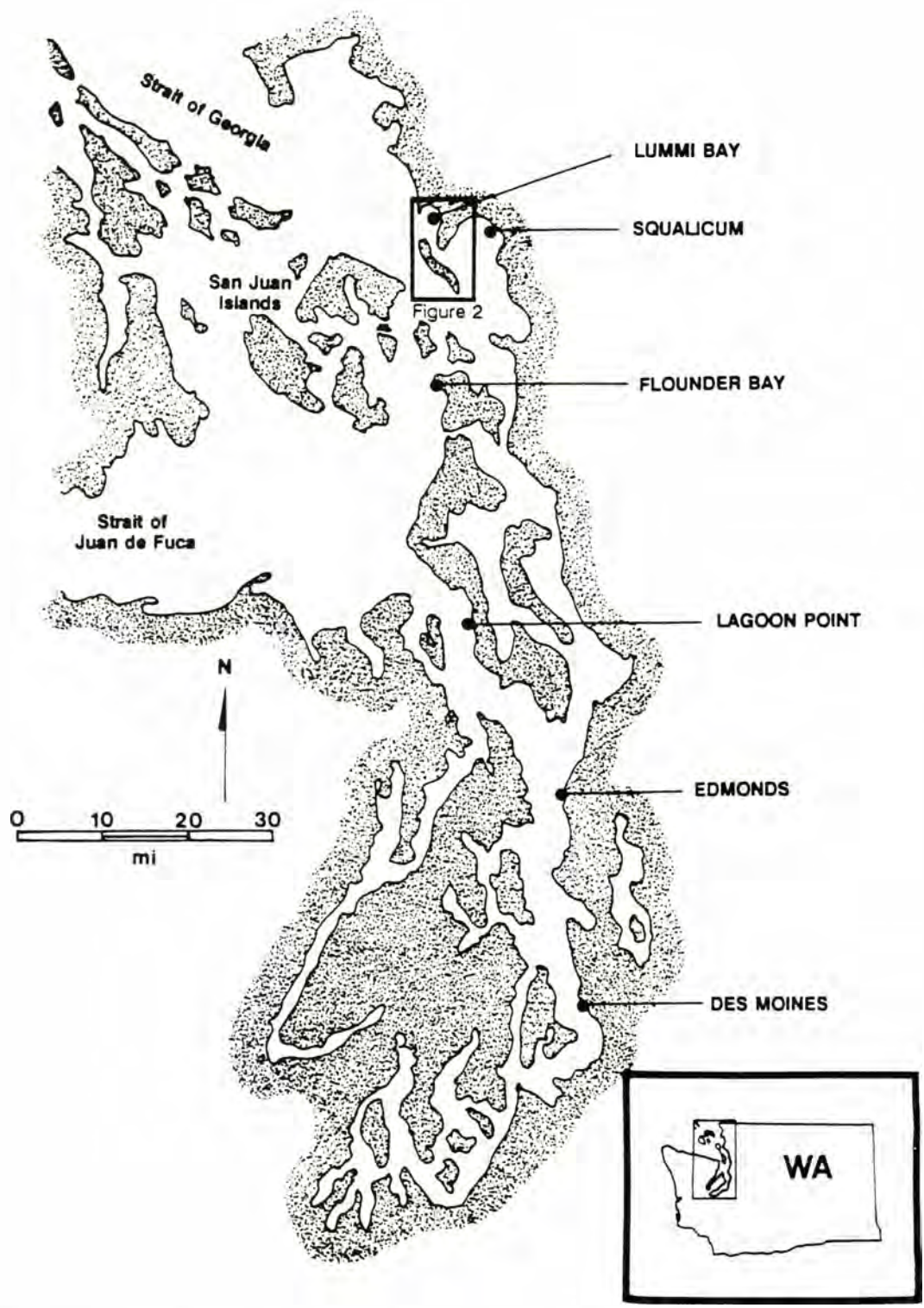


Figure 1. Location map of proposed Lummi Bay Marina and five other marinas to which it was compared.

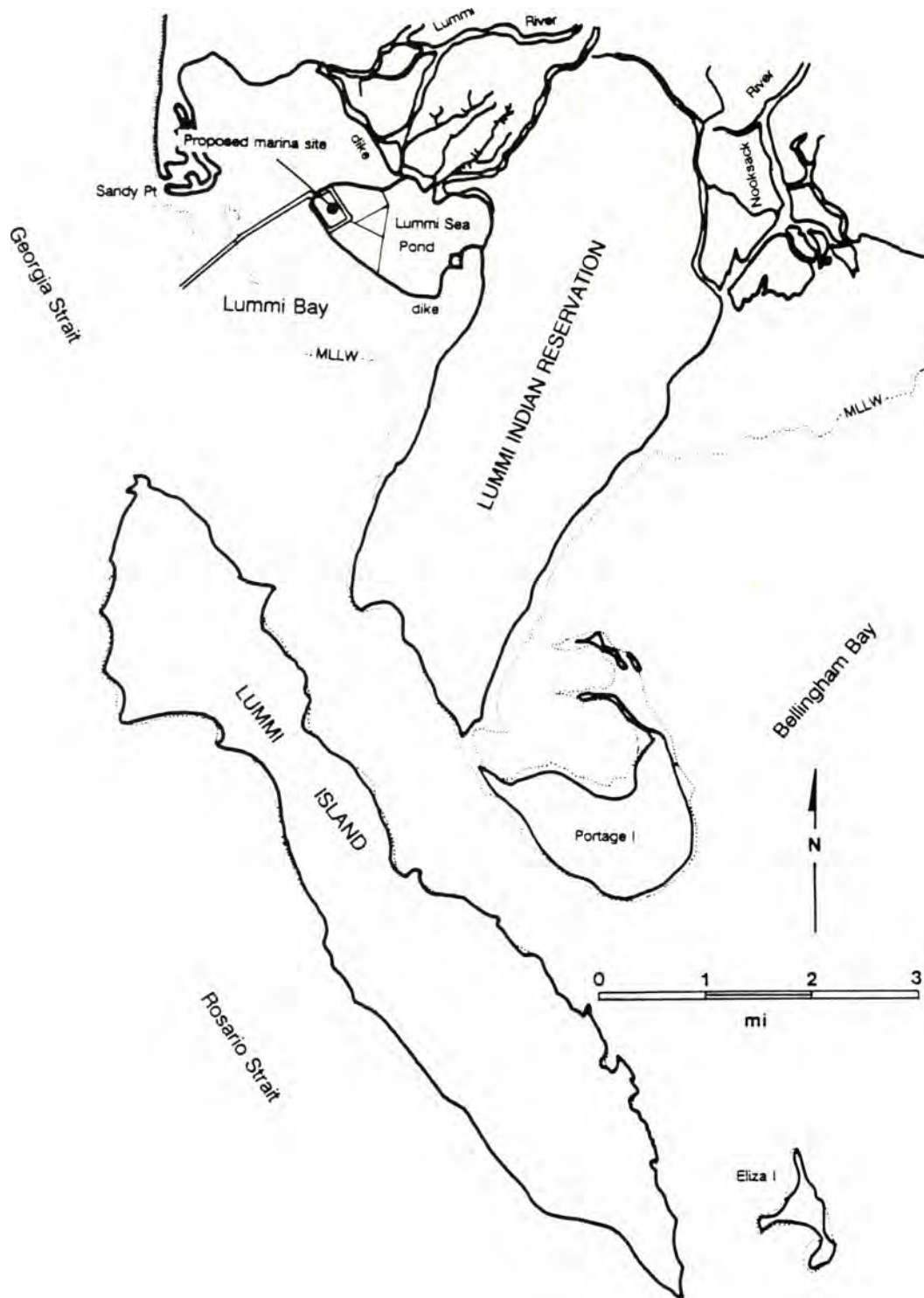


Figure 2. Map of Lummi Bay showing Lummi Sea Pond aquaculture site.

The mainland which surrounds Lummi Bay is composed of glacial or glacially-derived sediment. Glaciomarine drift, deposited from floating ice at the end of the last glaciation about 10,000 years ago, is the predominant sediment (Easterbrook, 1973). Sediment in Lummi Bay is generally silt to fine silty-sand, the latter being about 70% sand (U.S. Army Corps of Engineers, 1988). The project site has a 6 to 10 ft layer of organic-rich shelly fine sand which lies above beds of fine sands and sandy silts. (Customary U.S. units of measurement are used in this report in accordance with U.S. Army Corps of Engineers common usage. For conversion to metric units see Table 1.) All of the units contain varying amounts of clay. Beneath those beds, at about 107 ft below the surface, lies a compact clay. The U.S. Army Corps of Engineers (1988) interprets the clay as glaciomarine drift over which a sequence of deltaic and estuarine sediments from the Nooksack River has been deposited. The overlying deltaic-estuarine sediments are unconsolidated, while the glaciomarine drift may be more consolidated.

Since the diking of the Nooksack River shifted the fluvially-transported sediment into Bellingham Bay, depositional rates in Lummi Bay have been greatly reduced. Those reduced rates are offset by the sedimentation of Bellingham Bay, where depositional rates have dramatically increased (Bortelson et al., 1980; Easterbrook, 1973; Smelser, 1970).

TABLE 1.

Conversion factors:
 U.S. customary to metric (SI) units of measurement.
 (From Hudson et al., 1979.)

<u>Multiply</u>	<u>by</u>	<u>To obtain</u>
Inches	25.4	Millimeters
	2.54	Centimeters
Square Inches	6.452	Square Centimeters
Cubic Inches	16.39	Cubic Centimeters
Feet	30.48	Centimeters
	0.3048	Meters
Square Feet	0.0929	Square Meters
Cubic Feet	0.0283	Cubic Meters
Yards	0.9144	Meters
Square Yards	0.836	Square Meters
Cubic Yards	0.7646	Cubic Meters
Miles	1.6093	Kilometers
Square Miles	259.0	Hectares
Acres	0.4047	Hectares

Although fluvial sedimentation in Lummi Bay is almost non-existent, coastal sedimentation continues to have an impact on the bay. Sandy Point, an active spit, protects the northern portion of the bay from the Strait of Georgia's 90 to 100 mi fetch to the northwest (Figures 2 through 4). The spit is building to the south, with net shore-drift directions being southward on the western side of the spit, and northward on the eastern side (Jacobsen, 1980). The western side is the more active drift cell, so the spit progrades southward. The central portion of the Lummi Bay shoreline has been extensively diked, and the drift cells have been substantially altered. The bay's southern shoreline has a southward drift direction similar to that on the western

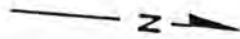


Figure 3. Oblique aerial view of Lummi Bay to west showing aquaculture pond (lower left) and Sandy Point (upper right). River channel is roughly where the access channel to the proposed marina would lie (photo by Russ Karns).

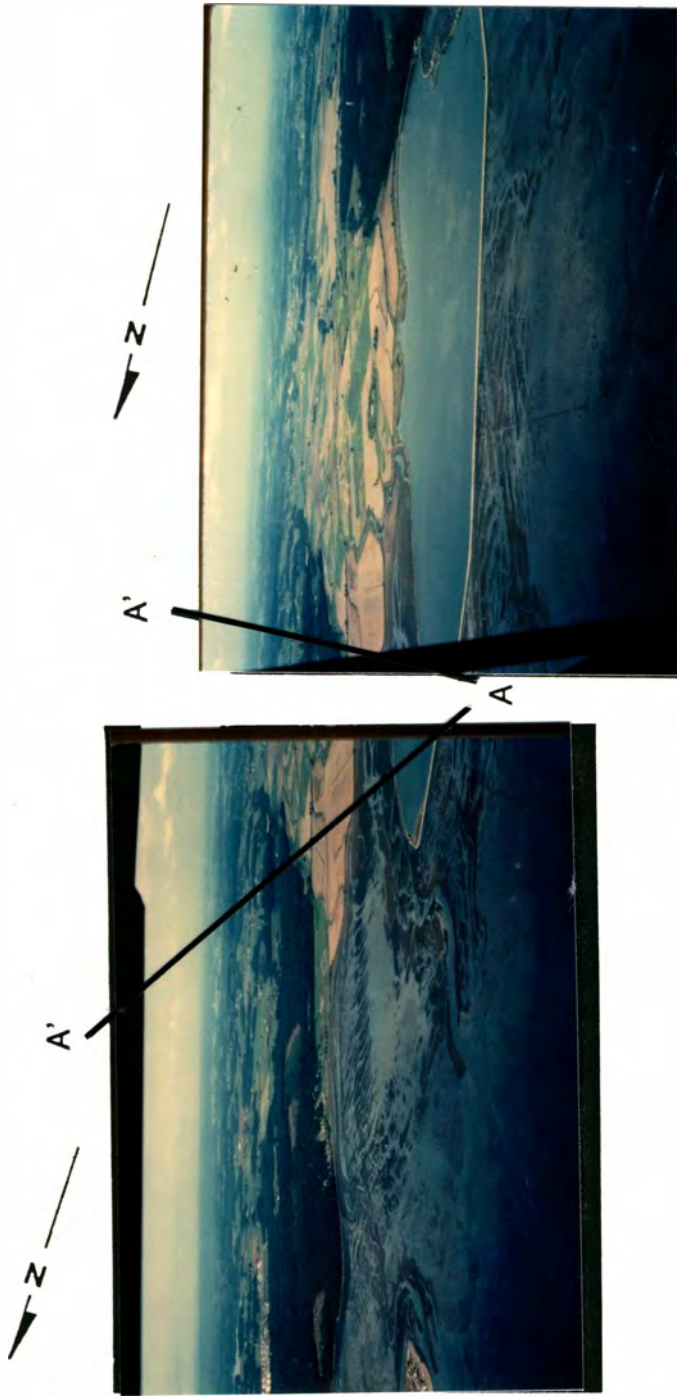


Figure 4. Composite oblique aerial view of Lummi Bay and surrounding landforms. Proposed marina site is situated in the aquaculture pond where photos overlap. Note drainage of Lummi River across the tidal flat. Sandy Point is at far left (photos by Russ Karns).

side of Sandy Point. A more complete discussion of net shore-drift can be found in Jacobsen (1980).

The maximum range of the tide at Lummi Bay has been estimated to be between 12.00 ft and -4.50 ft, ± 0.5 ft, mean lower low water (MLLW) (U.S. Army Corps of Engineers, 1988). This macrotidal range is typical of the region (Bird, 1984). Nearly the entire bay bottom, with the exception of some drainage channels, is exposed during extreme low water, while at extreme high tide the water depth across the bay is about 8 to 10 ft (U.S. Army Corps of Engineers, 1988).

The tides of the Pacific Northwest are typically of the mixed semidiurnal type. Mixed tides are those in which unequal highs or lows, or both, occur between successive cycles (Harris, 1981). The diurnal inequality occurs as the moon moves through its range of declination from the earth's celestial equator during the 27.2 day tropical month (Harris, 1981). Maximum diurnal inequality will occur during tropic tides, when the moon is at maximum declination, while minimum diurnal inequality occurs during equatorial tides, when the moon is at the celestial equator. In semidiurnal regions two high-tides and two low-tides generally occur during the 24 hour 50 minute lunar day, with the diurnal inequality being more prominent between the low tides. Spring tides occur during syzygy when the sun, moon, and earth are aligned. Neap tides occur when the moon is in quadrature, when the moon is 90 degrees from the alignment of the earth and sun.

Water that circulates in the inland waters of western Washington and British Columbia moves in from the Pacific Ocean. The Strait of Juan de Fuca is the major conduit between the ocean and the inland

waters with a small amount of water being introduced through Johnstone Strait north of Vancouver Island (Mofjeld and Larsen, 1984). The tide enters the Strait of Juan de Fuca as a long wave, forcing water to move through the system of channels and islands, and these tidal currents of the inland waters of Washington and British Columbia have been extensively studied (Mofjeld and Larsen, 1984). It is important to note here that a phase lag of up to 148 degrees and an amplitude change of the principal semidiurnal lunar-component of the tidal wave, called the M_2 component, is experienced as the wave moves through the San Juan Archipelago. Considerable energy is dissipated due to increased friction caused by water flowing through the multitude of small channels among the islands.

STATEMENT OF PROBLEM

Lummi Bay remained undeveloped, except for the shore dikes, until 1969, when construction of the aquaculture pond commenced in the bay (U.S. Army Corps of Engineers, 1988). The aquaculture pond was built on the tidal flat to enhance the Lummi Indian tribal economy through the production of fish and shellfish. Aquaculture has not been developed as extensively as originally planned, but the site remains the predominant man-made feature in Lummi Bay. The proposed marina would occupy the northwest corner of the Lummi Sea Pond (Figure 5). Modifications to accommodate the marina would reduce the 760-acre aquaculture pond by about 211 acres. The areas of the boat-moorage basin and berm each are about 25 acres, and the remaining 161 acres would be used for supporting facilities and a mitigation area between the marina and the remaining aquaculture pond. The berm, a ledge of unconsolidated sediment at the site, was designed to separate the dikes from the boat-basin and insure sediment stability beneath the dikes. A turning-basin and access-channel connect the boat-basin to deep water. The proposed channel would extend 7,300 ft across the tidal flat with a 100 ft bottom-width and dredged depth of -12 ft MLLW. The inner end of the channel would join the marina between two timber-pile breakwaters extending from the ends of the rock dikes. The breakwaters were designed to be open below the -2 ft MLLW level to allow for passage of fish. Additional pass-through features for fish were added to the breakwaters above the berm (Norman Skjelbreia, personal communication, 1989). The interior berm will extend around the perimeter, with the exception of the entrance, at the 4 ft MLLW level. The boat basin will be dredged to the depths shown

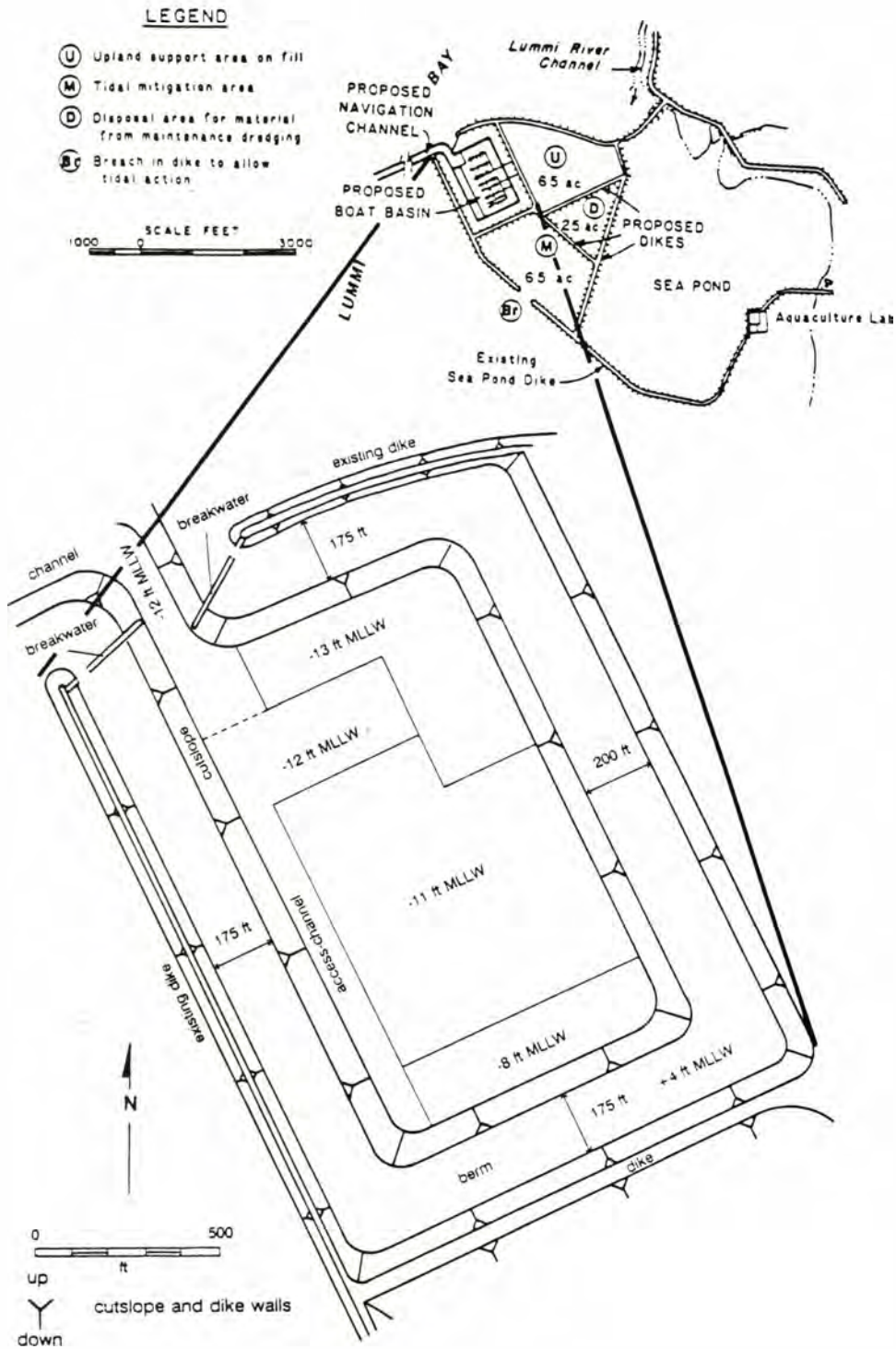


Figure 5. Plan of proposed Lummi Bay Marina showing terminology used in this study. Depths and berm widths are labeled. Datum for depths is Mean Lower Low Water (MLLW). (From U.S. Army Corps of Engineers, 1988.)

in Figure 5. The deepest region, dredged to -13 ft MLLW, would allow for access to the fuel dock and deeper-draft moorage. A -12 ft MLLW turning basin and channel along the western edge of the basin will give access to the shallower moorage, with moorage depths varying from -12 to -8 ft MLLW. About 1.47 million cubic yards of material would be dredged to complete the channel and boat-basin.

The design for the Lummi Bay Marina is distinct from other Pacific Northwest marinas. In general, marinas in the region are located adjacent to existing deep water, either in dredged lagoons or at the shore. The proposed access-channel to deep water for the Lummi Bay Marina would be the only means of continuous interaction between the marina and the Strait of Georgia. The berm of undredged tidal flat between the dike and moorage-basin is also unique to the project. Berms are not a consideration in dredged lagoons behind natural bars which serve as breakwaters, or in naturally-deeper marinas outboard of the shore, where dikes and breakwaters extend to depths greater than those found in Lummi Bay. Similarly, marinas with floating breakwaters do not need berms. As the design of the Lummi Bay marina is distinctly different from existing marinas, the effects of the differences in design needed to be investigated.

A concern over water quality has been expressed for all marinas. Since, by design, marinas are usually small, enclosed water-bodies, they may potentially become traps for water-borne pollutants. Studies continue to address the hydraulic behaviors of marinas (Nece and Forsyth, 1980). While numerical models such as that of Falconer (1980) have become more common as computing capabilities have expanded, those

methods remain most successful in analyzing the effects of tides and currents in larger estuarine or other coastal systems. Addressing the problems of small-scale construction projects using computer models is more difficult to do. In numerical analysis the depth component of a small marina becomes more important than its counterpart in a large estuarine system, because the former is proportionally much greater (Ronald Nece, personal communication, 1988). Numerical estuary models often vertically-average the depth dimension, thereby allowing a two-dimensional analysis of tidal currents (Thabet, et al., 1985). Accurate representations of small-harbor entrances, where turbulence is high, limit the practicality of numerical models. Boundary conditions also have a greater influence in small harbors than in larger systems. Physical models thus remain a useful method for studying tidal-flushing.

Marinas in the Pacific Northwest have been physically modeled in an effort to develop satisfactory designs (Nece et al., 1975; Nece et al., 1980). Water quality has become an increasingly important issue as population growth, accompanied by increased marine business and recreation, has stimulated development of the coastline. Part of that development has included a demand for more moorage space. While marinas are an obvious way to protect boats, they also act as havens for juvenile fish such as salmon from predation in the higher-energy environment of open water. Because marinas are also sources of pollution, tidal-flushing is incorporated into marina designs to help maintain acceptable water-quality. If a marina cannot be adequately flushed of pollutants - for example, of spilled fuel or sewage - concentrations will remain high in the interior water. Additionally,

during warmer summer months, algal-blooms can occur as the result of increased water temperature. The unaesthetic algal-blooms are accompanied by oxygen depletion as the algal population expands. Water, then, must be adequately exchanged to force the dilution of pollutants in a marina, to control temperature, and prevent deoxygenation; otherwise, stagnant and polluted conditions would prevail in the marina.

This study was carried out to examine the tidal-flushing behavior of the proposed Lummi Bay Marina. A physical model was used to investigate the problem for three reasons. First, as mentioned, the numerical-model approach was deemed impractical for reasons of simulation errors. To model turbulent conditions within the marina adequately using numerical methods would require extensive computing capabilities. Physical models, while generating less-quantitative data, better represent conditions found in a prototype by naturally accounting for transverse shear of the water. Second, the long history of physical modeling provides insights into problems which may develop during a study. Problems with physical models, such as those related to scaling, are more easily resolved than are those associated with numerical models of small marinas. Third, a field study could not be conducted because the study was predictive. Field investigation can yield data which may reveal the solution to a problem in existing marinas with inadequate water quality (Slotta and Noble, 1977). Provided that construction of the Lummi Bay marina proceeds, a field study is recommended to verify the present predictive approach.

The procedure used in the present study was to measure directly water conditions in the physical model to produce data to be used in the

calculation of exchange coefficients. The exchange coefficient is the average amount of water, expressed as a coefficient, removed from the basin during a tidal cycle, a tidal cycle being defined here as the period from one low water to the next low water (Nece et al., 1979). Exchange coefficients are useful in defining limits for water quality in marinas. The Washington State Department of Fisheries recommends minimum exchange coefficients of 0.25 (25%) for the maintenance of adequate water temperatures and 0.30 (30%) to keep dissolved oxygen levels high enough for marine life (U.S Army Corps of Engineers, 1988). The relationship of the exchange coefficient and its counterpart, the retention coefficient, is shown by the following equations:

$$E = 1 - R \quad (1)$$

and

$$R = (C_n/C_0)^{1/n} \quad (2)$$

where

E = average, per cycle, exchange coefficient,

R = average, per cycle, retention coefficient,

C_0 = initial spatial-average concentration of tracer in basin,

C_n = spatial-average concentration of tracer after n cycles,

n = integer number of tidal cycles.

The design of the marina's basin yielded an average tidal prism ratio (TPR) of 0.33. The TPR is a second method of estimating tidal-flushing abilities of a marina. The following ratio defines the TPR:

$$TPR = (V_{MHW} - V_{MLW}) / V_{MHW} \quad (3)$$

where

V_{MHW} = volume of basin water at mean high water,

V_{MLW} = volume of basin water at mean low water,

and mean high and low waters were averaged spring and neap tides.

Flushing efficiency is a measurement of the ability of a marina to flush itself. Flushing efficiency is used as a means of comparing the tidal exchange of the marina to that calculated using the tidal prism method (Nece et al., 1975). A flushing efficiency of 100% indicates similar behavior of a tidal system as calculated by the two methods. The flushing efficiency of the marina was predicted to be about 100% (U.S. Army Corps of Engineers, 1988). Calculation of the flushing efficiency was by the following method:

$$(E_{AV} / TPR) \times 100 \quad (4)$$

where

E_{AV} = average exchange-coefficient for the basin as determined from the model.

Previous physical-model studies of marinas of the Pacific Northwest have been based on repetitive, sinusoidal tidal oscillations and average tidal exchange-coefficients (Richey and Nece, 1972). Tides at Lummi Bay are not sinusoidal but are controlled by factors that cause a sizeable diurnal inequality and spring-neap variation. This study was designed to model spring and neap tidal conditions to determine their effects on tidal-flushing. In assessing the tidal-flushing ability of the Lummi Bay Marina, a qualitative approach supplemented the water-

sampling procedures, in that photography of the model documented circulation patterns. Water circulation in the proposed basin was predicted to be a single, counterclockwise gyre (U.S. Army Corps of Engineers, 1988). Formation of secondary gyres could trap water and prevent it from being flushed, with obvious negative consequences for water quality.

This study addresses the basin-design predictions of exchange coefficient, flushing efficiency, and water circulation patterns (U.S. Army Corps of Engineers, 1988); and compares them to the observed behavior of the model.

RELATED INVESTIGATIONS

The following review of selected literature outlines the types of studies available concerning the problem of water quality in Pacific Northwest marinas. A more complete bibliography can be found in Nece and Forsyth (1980).

Richey and Nece (1972) studied four different designs for a proposed marina at Lake Crockett on Whidbey Island using a physical model similar in scale to the present model. Using Rhodamine-B, a fluorescent dye, the gross exchange coefficients were determined for the different designs. Circulation patterns were studied by observing visible dye during the tests. After tidal cycles were simulated and the water in the model was artificially mixed, four samples were taken and fluorescence was measured. Fluorescent dyes were, then, an early means of quantifying flushing abilities.

Ward (1973) developed a method of photographically quantifying dye concentrations, using an organic blue dye which was injected into physical models and photographed. Dye concentration was calibrated and measured using a microdensitometer. This method was applied as a way to avoid using unstable fluorescent dyes. A second benefit was the ability of a microdensitometer to measure and record dye concentrations during simulations.

Four Pacific Northwest marinas were studied by Nece et al. (1975) to help establish flushing criteria for marinas. Rhodamine-WT fluorescent dye was used, although Ward (1973) had suggested that fluorescent tracers were inadequate. Water in the four marinas was sampled for a variety of biological, chemical, and physical properties

pertaining to water quality. Vertically-distorted physical models of each marina were employed to correlate the field data with flushing characteristics determined using fluorescent dye. Two samples per simulation were taken from the fully-mixed models and measured in a fluorometer to obtain gross flushing-coefficients. The dye was susceptible to "quenching" by free chlorine in the water supply, and an attempt was made to minimize the effect by adding sodium thiosulfate to counteract it. Rhodamine-WT is also susceptible to decay through heat and sunlight and thus proved to be a less-than-adequate tracer.

Richey and Smith (1977) studied a proposed expansion of the Birch Bay Marina. Fluorescent dye was again employed, in conjunction with photodensitometric and photographic methods. Gross exchange-coefficients were determined using methods similar to those of Nece et al. (1975). Variations in water quality through the tidal cycles were measured using a photodensitometry method similar to that of Ward (1973). Photography was used to study circulation patterns. An analysis of velocity in the channel into the prototype supplemented the flushing and circulation studies.

A study of the effect of planform geometry of marinas on tidal flushing (Nece et al., 1979) expanded on the flushing criteria of Nece et al. (1975). Physical models of several different rectangular configurations were studied using photodensitometry to measure dye density. Exchange coefficients were contoured so that basin-wide water quality could be measured. Nece et al. (1979) concluded that marinas with a length-to-width ratio between 1:3 and 3:1 would flush most efficiently. Entrances positioned centrally on the outer breakwater

would force the best circulation of water inside a marina. As part of the study, Nece et al. (1979) modeled identical, repetitive sine-like tides at LLW to minimize currents and allow for better replication.

Nece et al. (1980) collected field data and physically modeled five marinas to more accurately document flushing and circulation. The marinas were modeled under conditions similar to those of Nece et al. (1979). Exchange coefficients were measured using a photodensitometer. New exchange coefficients were calculated for the marinas, all of which had been previously studied. The more conservative values were a result of measurements being made at LLW, a practice described by Nece et al. (1979).

Studies of Pacific Northwest marinas have centered on measuring exchange coefficients in physical models using fluorescence and photodensitometry, sometimes including field studies for comparison. The method used in the current study utilized concepts of previous workers and offers a useful variation in methodology.

METHODS

Scale Models

Scales were chosen for construction of the physical model according to Froude scaling relationships (Hudson et al., 1979). These relationships are a means by which to simulate prototype conditions in a model. A variety of formulae are used to describe conditions of flow in hydrodynamic systems, the most common being the Mach-Cauchy, Weber, Reynolds, and Froude numbers. Tidal systems are modeled using a ratio of model-to-prototype Froude numbers because gravitational forces predominate (Hudson et al. 1979). As a result, the Mach-Cauchy, Weber, and Reynolds numbers, which respectively include terms for inertial forces, surface tension, and viscous forces, need not be considered (Hudson et al.,1979). The dimensionless Froude number, F_n , is expressed as

$$V / (gL)^{1/2} \quad (5)$$

where V = velocity,
 g = gravitation,
 L = length.

Similitude is achieved between the model and prototype using the Froude Model Law, defined as:

The required quality of the Froude number, model-to-prototype, which indicates that the ratio of gravitational to inertial forces in a model should equal the corresponding ratio in the prototype... (Hudson et al., 1979).

It is noted that while the above definition includes inertial force, it is gravitational force that is predominant, and inertial force is generally not considered in terms of the Froude number.

The components that were scaled in this study were horizontal length (L_H), vertical length (L_V), and tidal-time (T_t). Table 2 lists the components and scale ratios used for this study. In Table 2 note that the expression of tidal-time in length terms yielded a calculation of scaled tidal-time.

TABLE 2.
Relationships of scaled dimensions between
model and prototype of the
Lummi Bay Marina.

<u>Characteristic</u>	<u>Dimension</u>	<u>Model-to-Prototype Ratio</u>
Horizontal Length	L_H	1:500
Vertical Length	L_V	1:50
Tidal-time	$T_t = L_H/L_V^{1/2}$	1:70.7

The scaled vertical and horizontal lengths gave the physical model geometric similarity to the proposed marina. The time required for the 12.42 hr semidiurnal tidal-period was scaled using the tidal-time equation in Table 2 and yielded a scaled semidiurnal tidal-period of 10.54 min, thus giving kinematic similarity between model and prototype. Vertical distortion was used to minimize the effects of bed roughness and fluid surface-tension. Physical models which are vertically-distorted are more dynamically similar to their prototypes for the reason of minimizing effects of viscosity, surface tension, friction, and turbulence. While absolute similitude between model and prototype cannot be achieved, vertical distortion should not affect modeling, where water flows horizontally as a long wave of greater magnitude than the water depth (Hudson et al., 1979). Additionally, scales used in

this study have been shown through previous work to replicate adequately prototype conditions (Nece et al., 1975; Nece et al., 1980). Effects of boats, slips, wind, and water stratification were not considered in this study.

Design of the Model

The design of the model used in this investigation differed from the physical models of Nece et al. (1979) in four ways: depths proposed for the marina were included in the physical model; a berm around the perimeter of the model moorage-basin was included; the walls of the model were sloping rather than vertical; and tidal characteristics were modeled to better represent prototype conditions. Nece et al. (1979) addressed the relationship of planform geometry of small harbors and tidal-circulation where the depth of each modeled basin was constant and uniform. Boat-basins of constant depth are common in the Pacific Northwest, although those depths vary between individual marinas. The proposed Lummi Bay Marina was designed with variable depths in response to the needs of the project and the costs involved in dredging to a uniform deep depth. The physical model of the current study was depth-contoured to reflect the proposed design (Figure 5).

A berm was included in the proposed design to give structural support to the dikes and wall surrounding the moorage-basin (U.S. Army Corps of Engineers, 1988). The berm would vary in width, from 175 feet on the north, west, and south edges, to 200 feet on the east edge, reducing the interior volume of the marina that could be used as a moorage-basin (Figure 5). Using data published by the U.S. Army Corps

of Engineers (1988), the berm in the model was designed to +4.0 ft MLLW, which was assumed to be the elevation of the tidal flats for this study. The Lummi Bay Marina, while having length-to-width ratios within the limits suggested by Nece et al. (1979), will experience a change in water water-surface area due to tidal fluctuation. The berm will cause an increase or decrease in water-surface area and volume as tides move water above or below the +4.0 ft elevation respectively.

Vertical-walled models were used in previous studies of marinas in the Pacific Northwest (e.g., Nece, 1984; Falconer, 1980). In this study the walls of the physical model were sloped to reflect the conditions at the proposed marina. The model was distorted vertically causing the model walls to be steeper than those of the prototype, but the angle of the walls remained more representative of the proposed marina design than vertical walls would have been. As with the berm, the effects of sloping walls in the proposed marina was examined in order to determine how water circulated.

Tidal conditions were modeled after those found at Lummi Bay. Two unequal highs and lows occurred in the course of each lunar day. Each simulation began at lower low-water (LLW). Spring-tide simulation progressed through a larger flood-tide to higher high-water (HHW), a smaller ebb-tide to higher low-water (HLW), a second, smaller flood-tide to lower high-water (LHW), and a second, larger ebb-tide which returned the water level to LLW. Simulated neap-tides differed in sequence of highs and lows from the spring-tide simulation by initially having a smaller flood-tide from LLW to LHW, a smaller ebb-tide to HLW, flooding

with a second, larger tide to HHW, and ebbing back to LLW with a larger ebb-tide. Figures 6 and 7 display the tidal curves for each simulation.

Model Construction

Polystyrene insulating-foam was chosen as the construction material because of its adaptability and the ease with which it can be worked. Construction adhesive and acrylic caulk were used for bonding and sealing the foam. Acrylic-latex paint gave a uniform white coating over the interior of the physical model. Breakwaters at the marina entrance were simulated using sheet acrylic (figure 8). To separate water within the model from exterior water, a sheet acrylic dam was constructed and edged with modeling clay as a seal. The breakwaters, as designed in the Final Project Report and Environmental Impact Statement (U.S. Army Corps of Engineers, 1988), are open below the -2.0 ft MLLW elevation to allow for fish passage. The model was designed accordingly. The bottom edges and vertical sides of the breakwaters were designed to induce turbulence in the water and prevent water stratification. Three vertically-positioned cross-shaped posts were installed in the channel between the tide generator and physical model to simulate mixing of water in the channel (Figures 8 and 9).

Design and Construction of the Tide Generator

Tide generators are varied in design (Hudson et al., 1979; Nece, et al., 1979). The tide generator used in this study consisted of a waste-weir which was controlled by electrically-driven rotating cams (Figures 9 and 10). Two sets of cams were designed and constructed, one

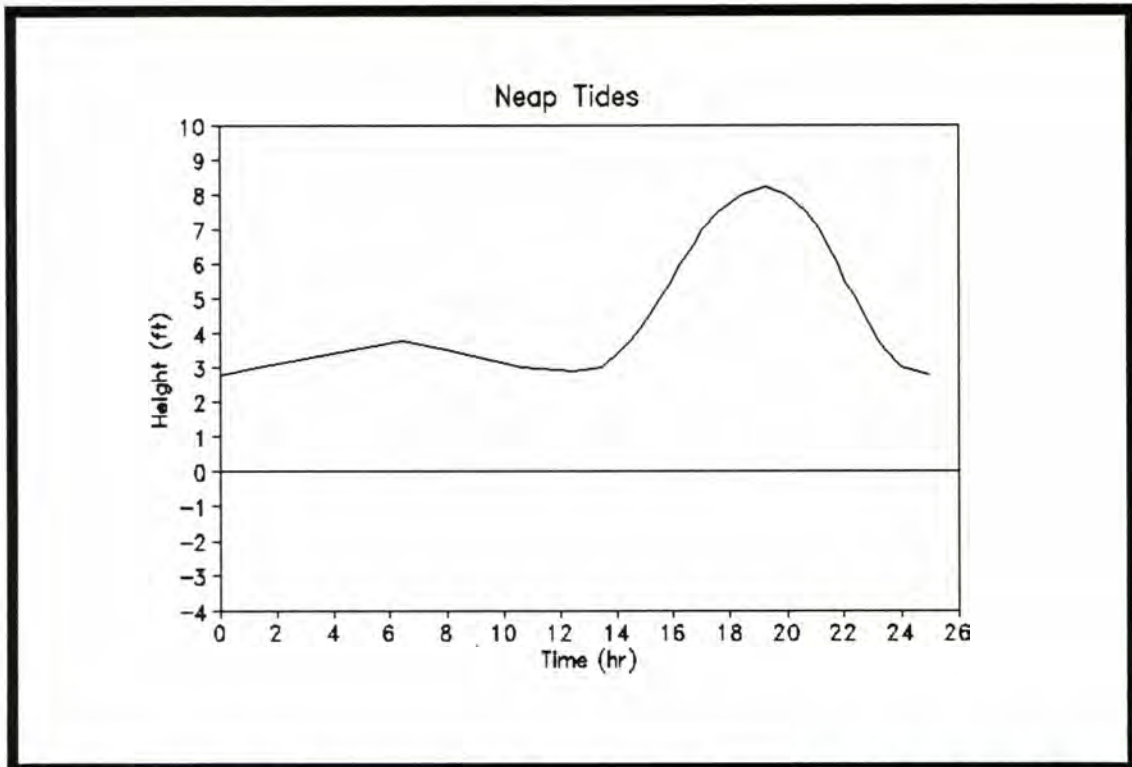


Figure 6. Neap-tide curve used for physical-model simulation of tides at Lummi Bay. Units are expressed in terms of the prototype.

each for the spring and neap simulations. A transmission system reduced the motor speed and rotated the cams one revolution every 10.54 mins. At each slack-tide a cam-follower attached to the waste-weir was moved to the cam representing the next tide, flood or ebb, in the desired sequence. During the change of cam positions the connecting-rod between the cam-follower and waste-weir was braked to prevent any change in tidal height.

Between the waste-weir and model a metal box housed the water supply-manifold. A layer of coarse gravel baffled the water supply and prevented turbulence from affecting the modeling process. The physical model and tide generator were attached and sealed together to prevent any leakage or movement. A second baffle, installed in front of the

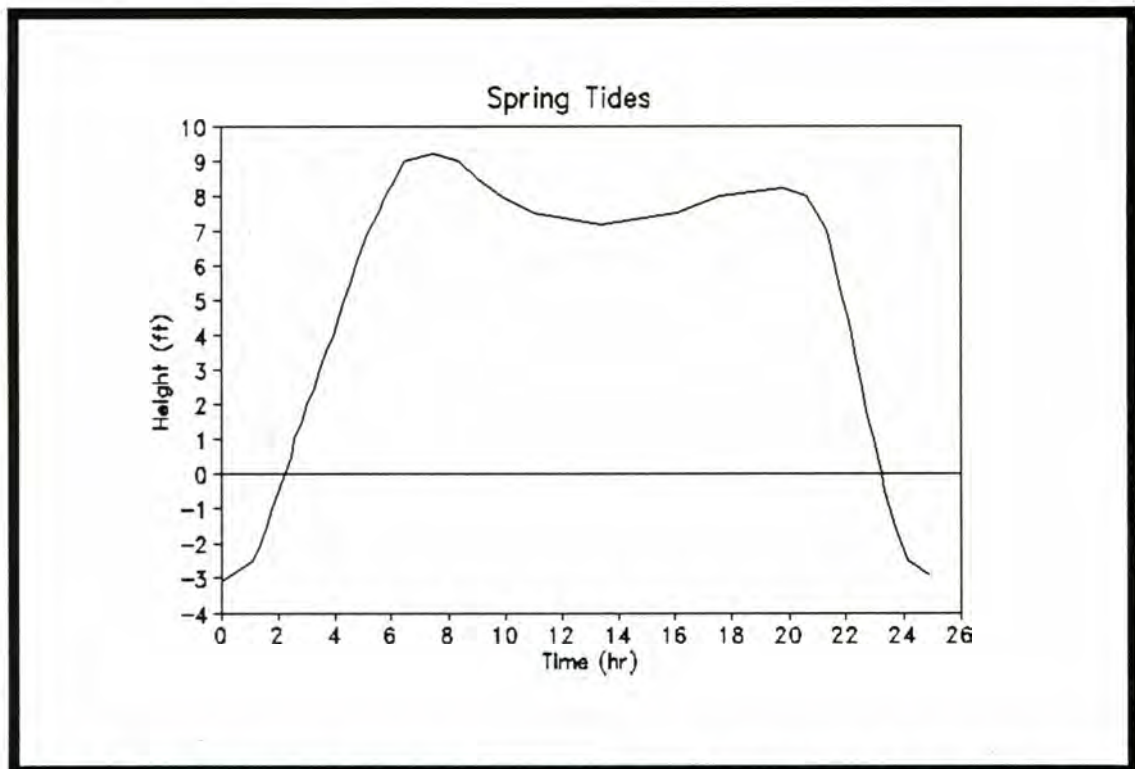


Figure 7. Spring-tide curve used for physical-model simulation of tides at Lummi Bay. Units are expressed in terms of the prototype.

waste-weir, slowed surface flow caused by the drop in elevation-head at the weir.

Calibration Procedures

Calibration was performed to insure that the apparatus was operating properly. The three types of calibration procedures are discussed below.

Calibration of Timing

The control of tidal fluctuations in the model involved a system of cams used to raise and lower the waste-weir. High or low tide as controlled by the cams was determined as a position on a cam on which

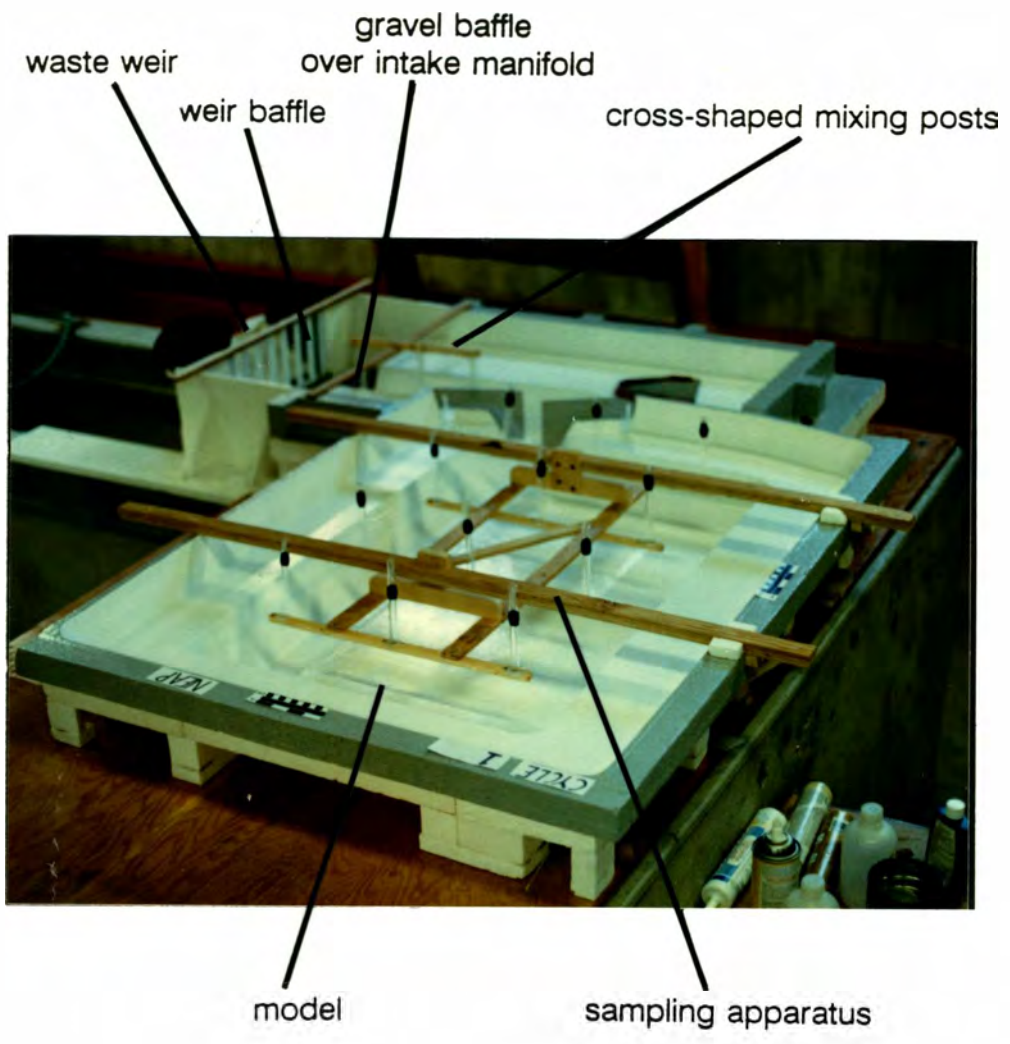


Figure 8. Photograph of the Lummi Bay Marina physical model.

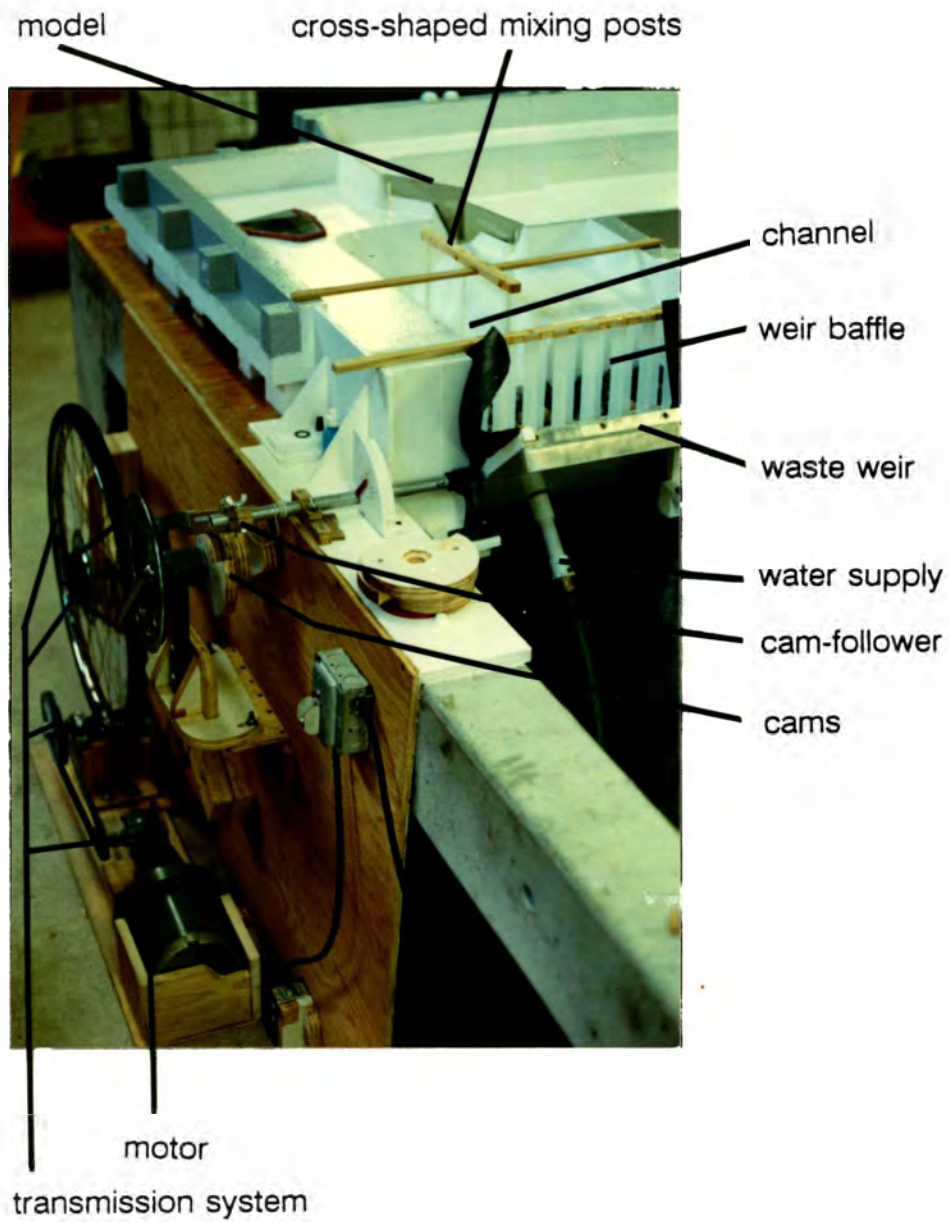


Figure 9. Photograph of the tide-generator used in this study.

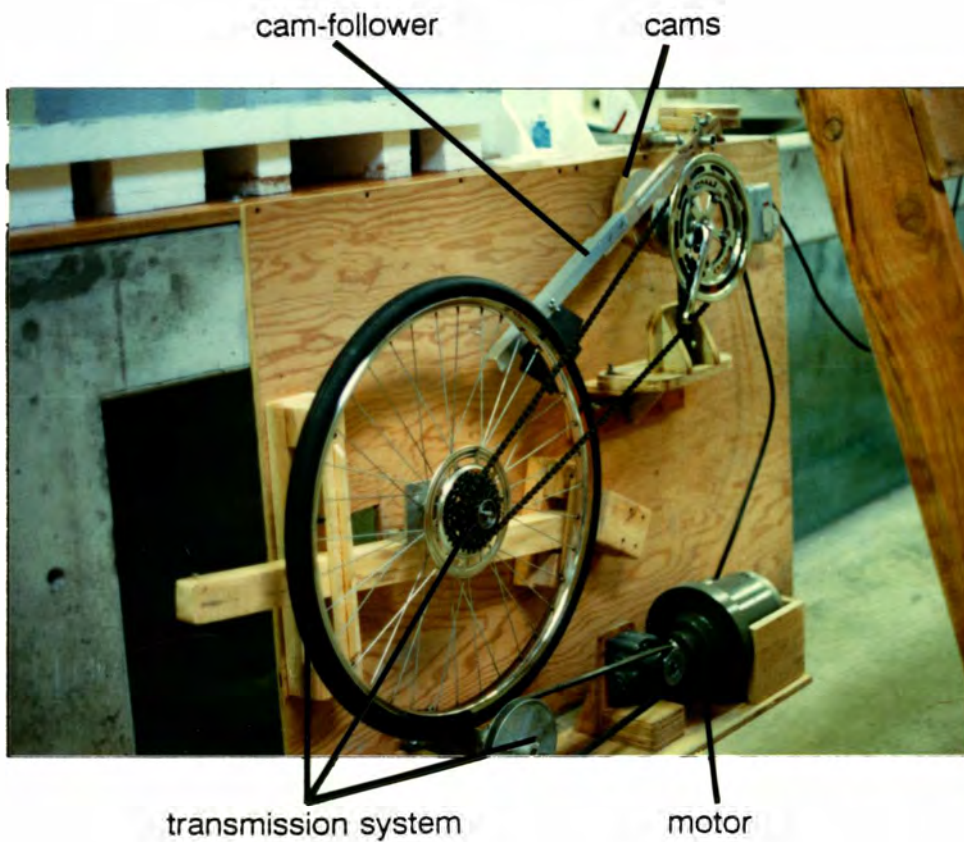


Figure 10. Photograph of the tide-generator from another angle showing motor, transmission system, cams, and cam-follower.

the cam-follower rested. These positions were determined by a line drawn on the cam-face perpendicular to, and through, the axis of rotation of the cams. Each high or low tide occurred when the cam-follower was oriented perpendicular to the lines drawn through the center of rotation. At those times the cam-follower was either at a minimum or maximum height. The eccentric nature of rotation dictated that each of the points occurred at something other than 180 degrees of rotation. Consequently, the point of contact on the cam-follower changed as rotation occurred, as did the degrees of rotation between tides. In essence, the tide generator does not precisely represent repetitive, sinusoidal tides but is more representative of tides at Lummi Bay.

Calibration of Height

Two sets of cams were constructed to represent spring and neap tidal heights. Tidal heights were measured to the 0.1 ft level of the prototype, consistent with the degree of precision described by Hudson et al. (1979). Consistency of water height in the model between like simulations was checked by running repetitive tests. Intervening 0.5 ft tidal levels and times between high and low tides were recorded as a means of inspecting curve shape. Results for averaged high and low tides are represented by Figures 6 and 7. All data-collection trial runs within the spring and neap simulations were consistent with each other.

Dye Selection and Calibration

A Bauch and Lomb Spectronic 21 spectrophotometer was used for the measurement of dye concentrations in the tidal simulations. The dye which was selected was Mrs. Stewart's Laundry Bluing because it is safe, inexpensive, and readily available. Bluing absorbs a distinct light wavelength and contrasts well to the surface of the model and was, therefore, effective in spectrophotometric, as well as photographic, analysis.

Bluing was analyzed for light-absorbance characteristics using an IBM model 9420 double-beam spectrophotometer. Light at the 680 nanometer (nm) wavelength was strongly absorbed by bluing, so all subsequent analyses used that wavelength (Figure 11).

After determining the distinct 680 nm absorbance wavelength of bluing, a sample solution of bluing and water was tested to determine whether bluing reacted according to the Beer-Bougouer-Lambert Law, commonly referred to as Beer's Law (Christian, 1977). Beer's Law correlates the amount of light transmitted through a material to the concentration of that material through the equations:

$$A = abc \quad (6)$$

and $T = 10^{-abc} \quad (7)$

where $T =$ transmittance, expressed as a percentage,
 $A =$ absorbance of an absorbing material,
 $a =$ absorbtivity, a proportionality constant dependent on the wavelength and the nature of the absorbing material,
 $b =$ sample-cell path length used in measurement of the material,

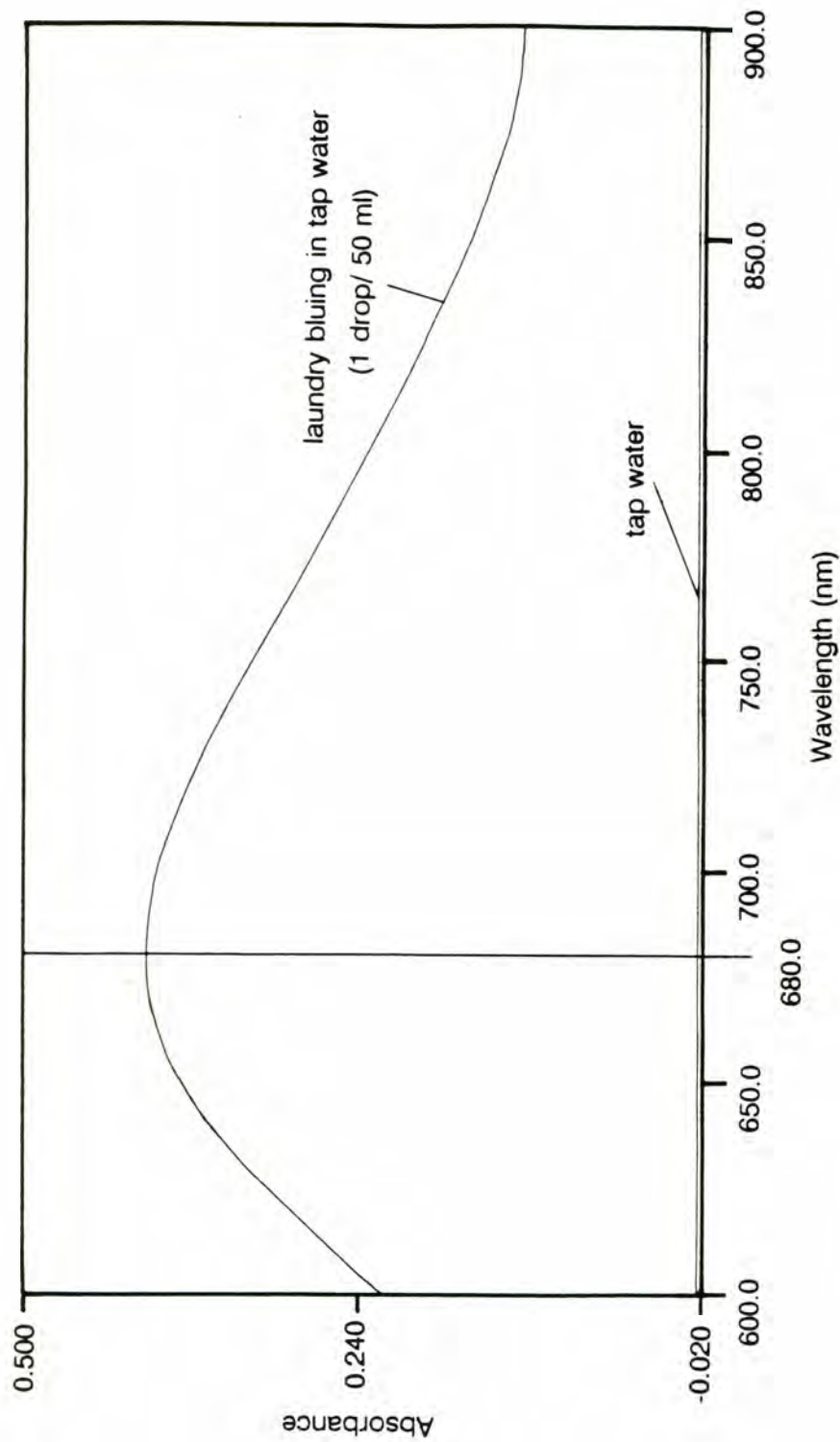


Figure 11. Wavelength vs absorbance of Mrs. Stewart's Laundry Bluing as detected by the IBM double-beam spectrophotometer showing strong light-absorbance by bluing at the 680 nm wavelength. Note that the curve of the tap-water blank solution is also plotted.

c = concentration of the absorbing material.

Both transmittance and absorbance were measured directly from a solution using a Bausch and Lomb Spectronic 21 spectrophotometer.

A solution of bluing in tap water was prepared by diluting 4 milliliters (ml) of bluing in 2 liters (l) of water. This solution was considered to be the approximate maximum-concentration at which bluing and water would react according to Beer's Law (Clinton Burgess, personal communication, 1989). Subsequent dilutions were then made of the solution and tap water. The known concentrations of the solution and its dilutions are shown as the x-axis in Figure 12. Clear tap water was used as a blank solution to set the instrument at 0 absorbance (100% transmittance) prior to measurement of the known dilutions of bluing-tap water solution. The coefficient of determination, a measure of variation of one variable determined by the variation of the other (Sokal and Rohlf, 1981), was $r^2 = 0.99991$, indicating that the relationship between bluing-concentration and absorbance is linear. Slope of the line was calculated as 0.99, with the y-intercept at 3.83×10^{-3} . For experimental purposes, the 4 ml bluing to 2 l tap water solution was then used as the maximum concentration for initial concentrations of bluing. Spring-tide simulations used an initial bluing dosage of 40 ml, and neap-tide simulations used 80 ml of bluing: smaller dosages were used for spring tides because less water was present in the model at spring LLW than at neap LLW. Bluing dosages were calculated for LLW basin-volumes, allowing initial concentrations of bluing-water mixtures to be within the limits to react according to Beer's Law.

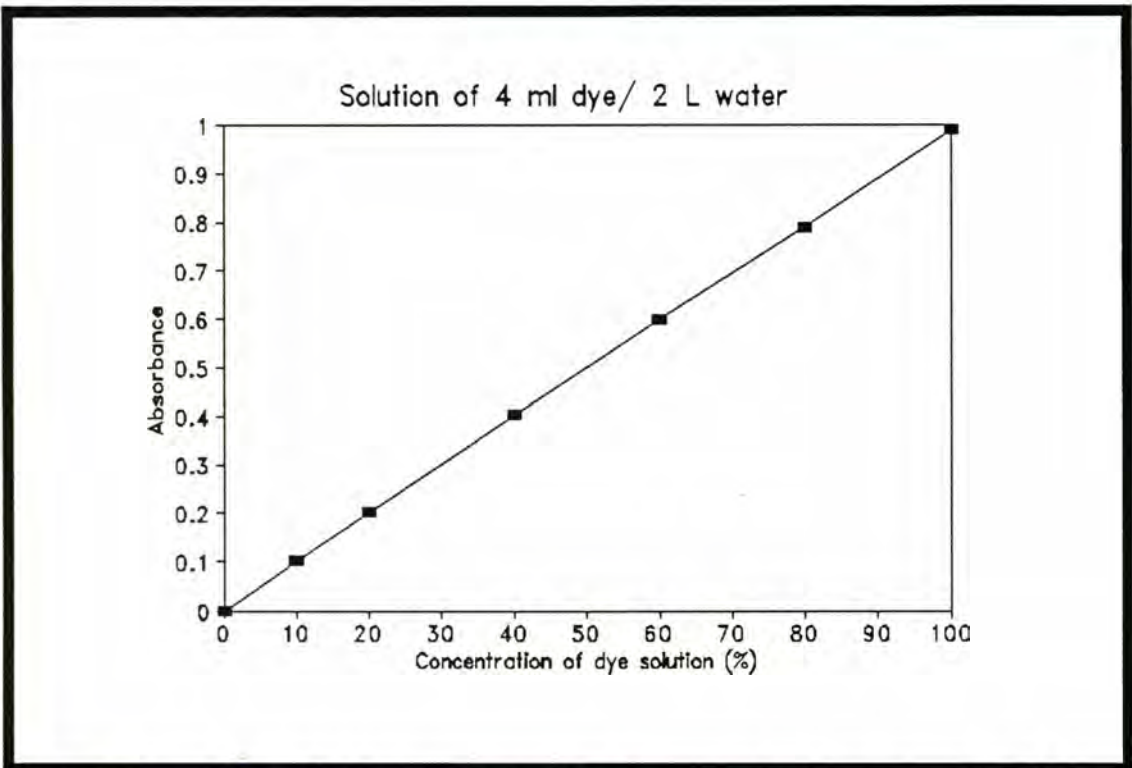


Figure 12. Plot of bluing concentration vs absorbance. The linear relationship indicates that bluing absorbs light as predicted by Beer's Law.

Quantitative Methods

Two sets of tidal ranges were chosen to represent spring and neap tides using tide tables (U.S. Dept. of Commerce, 1988). These ranges do not represent absolute maximum and minimum ranges of regional tides but represent approximate ranges which might be expected to occur annually. Table 3 lists ranges of the tides in actual and scaled terms.

TABLE 3.

Tidal heights used in the physical model of the proposed Lummi Bay Marina.
(Datum is MLLW)

<u>Type of Simulation</u>	<u>Prototype (ft)</u>	<u>Model (in)</u>
Spring Tide	LLW -3.1	-0.7
	HHW 9.2	2.2
	HLW 7.2	1.7
	LHW 8.2	2.0
Neap Tide	LLW 2.5	0.6
	LHW 3.1	0.7
	HLW 2.5	0.6
	HHW 8.0	1.9

Ten trial runs were conducted for each tidal simulation. Each simulation was initiated by filling the model with water to HHW in order to wet the entire surface of the basin, followed by spilling off water to LLW. Flushing the water supply reduced the chances of a large temperature variation and related stratification effects.

Sampling tubes for water collection were set to collect a column of water extending from the surface to the bottom of the model to reduce the effect of water stratification. The twelve tubes were inspected and installed in a sample rack in the raised position while the model was filling. The rack was prepared before a run so that it could be quickly placed over the model at the completion of the run. The tubes were sequentially numbered from 1 to 12 to insure that they would be inserted in the same sequence for each trial-run.

All runs began and ended at LLW with water samples being taken after the end of the fourth ebb-tide. The cam-follower (Figures 9 and

10) was positioned over the initial LLW point on the cam and secured. The dam was placed in the model entrance between the breakwaters (Figure 8) and a sample of clear water was taken. Laundry bluing was added to water in the model and was stirred until it was uniformly mixed. A sample of the initial dye-concentration was taken after mixing. Water movement in the model was allowed to calm for a period of at least four minutes. When no movement in the model was observed the dam was removed and the tide generator and a stopwatch were simultaneously started.

During each simulation, tides were observed and details recorded. At each tide change, the tide generator was stopped while the cam-follower was repositioned over the correct cam. Stopping the generator served to keep the cam and cam-follower properly oriented during the tide change and also simulated slack-tide conditions. Slack-tide times averaged 15.0 sec for spring simulations and 15.8 sec for neap simulations. In the case of neap-tide simulations only three cams were used. Consequently, the HHW tide change did not require a repositioning of the cam-follower but the generator was stopped for 15 seconds to simulate slack-water conditions and to maintain similar conditions. As the cam-sets for each tidal type were representative of one lunar day (two tidal cycles), the generation of two lunar days (four tidal cycles) was completed by running a series two consecutive lunar days.

When the water level was low enough on the final ebb-tide, the sampling rack was installed over the physical model and readied for use. At the end of the ebb, the tide-generator and stopwatch were simultaneously stopped, and the dam was replaced at the model entrance. As quickly as possible each tube was inserted vertically, beginning with

tube 1 and ending with tube 12. In spring-tide simulations it was observed during practice runs that not enough water was collected in tubes 4 and 5 due to shallow conditions. This problem was remedied by placing auxiliary tubes next to them to increase sample size.

After all of the sample tubes were lowered, each was stoppered to trap the contained columns of water within them. Each tube was then removed, in order, from the apparatus and the water was collected in labelled bottles. When all of the samples were taken, the empty rack was removed from the model and the remaining water was mixed to uniform color; a final sample was then collected. The empty tubes and model were washed as soon as a simulation was completed to reduce any contamination problems in future experiments. The model was then dried to prevent deterioration.

Measurement of absorbance of the bottled samples took place within a day of collection to minimize any chance of bluing deterioration. Most samples were measured on the day of collection. A Bausch and Lomb Spectronic 21 spectrophotometer was turned on ten minutes prior to use to assure that all components were at operating temperature. All samples were vigorously shaken to insure uniform mixing. Each was then placed in optically-correct measurement tubes supplied with the spectrophotometer. Before each tube was inserted in the instrument it was agitated again to mix the sample. If air bubbles were present they were loosened from the walls of the tubes by gentle tapping to reduce the chances of spurious readings.

Measurement proceeded with a primary reading of the clear water sample, at which time the instrument was set to an absorbance value of 0

(100 % transmittance), for the 680 nm wavelength. Measurements of the initial bluing-water sample, the 12 sample-points, and the artificially-mixed sample were completed, and each reading was recorded as both absorbance and transmittance. A final measurement of the clear water sample was taken to insure that no drift in the spectrophotometer had occurred. Immediately following measurement all glassware was thoroughly rinsed to prevent contamination of subsequent runs. Absorbance values for each run were then tabulated.

Qualitative Methods

During simulations for water collection, notes were kept regarding circulation and other phenomena. Observations were made concerning circulation-gyre formation, flood and ebb tidal action, and any phenomenon during a simulation which could affect the results. Separate runs were also conducted to record photographically the circulation of water during spring and neap simulations. Results of those simulations are discussed in the following section.

RESULTS

Flushing Coefficients

The calculation of values for mean flushing coefficients, E_{av} , was completed using the method described in the previous section. Ten trial-runs of each tidal simulation showed that replication between similar runs was consistent. The investigation was designed to include an analysis of variance. A completely-randomized design with a significance level of 5% was the method of analysis. The difference between the two simulations was highly significant. Spring-tide trial runs had a mean exchange coefficient of $E_{av} = 0.50$, and neap-tide trial runs had a mean exchange coefficient of $E_{av} = 0.22$. Figures 13 and 14 show values at sample locations for each simulation averaged over ten trial runs. The exchange coefficients, tidal-prism ratios, and flushing efficiencies are compared to those from other Pacific Northwest marina physical-models in figures 15 through 17. The five other marinas to which Lummi Bay is compared were modeled using LLW photodensitometric measurements for calculation of exchange coefficients (Nece et al., 1980). Results of studies which used HHW-derived exchange coefficients were not considered for comparison here.

Spring-Tide Trial Runs

Spring-tide trial runs were initiated under calm conditions at LLW. As the tide flooded, a current began to flow into the marina. The current initially flowed straight in, but curved toward the center of the marina as it continued. The berm controlled one side of the current, but a counterclockwise circulation-gyre began to move water

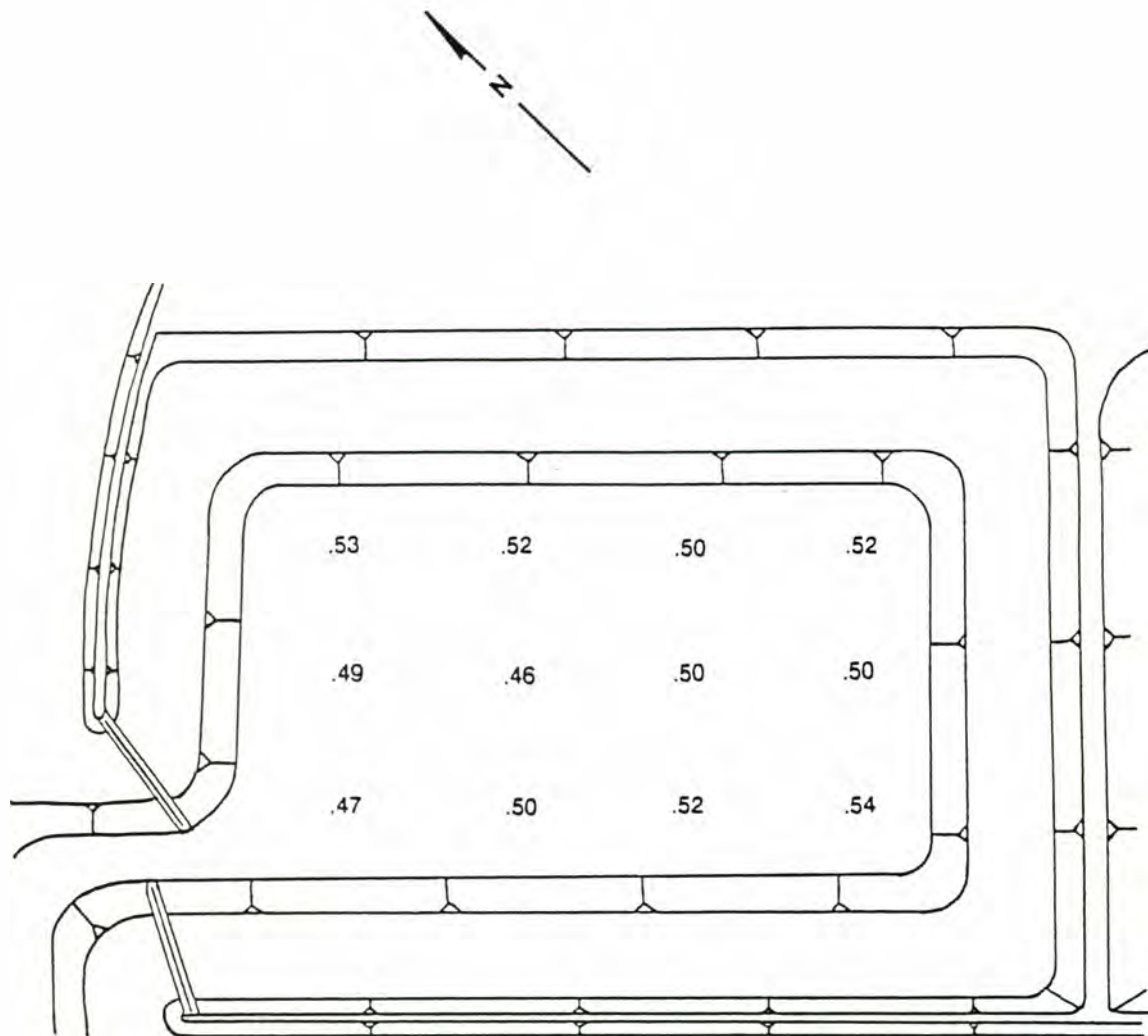


Figure 13. Mean local exchange-coefficients for sample locations from 10 spring-tide trial runs. Each trial run simulated two lunar days (four tidal cycles). Water was sampled at LLW. Mean exchange for spring-tides was $E_{av} = 0.50$.

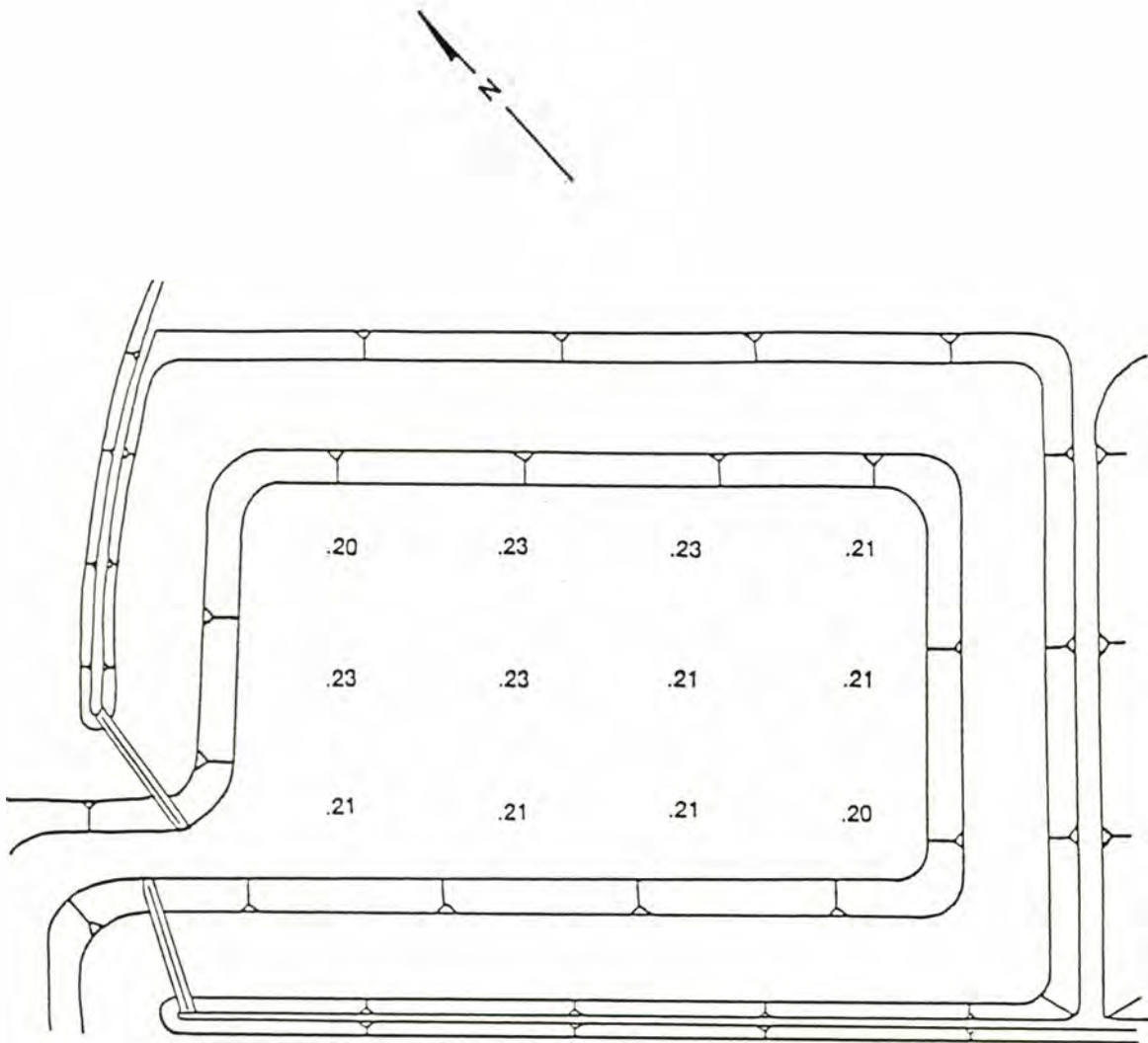


Figure 14. Mean local exchange-coefficients for sample locations from 10 neap-tides trial runs. Each trial run simulated two lunar days (four tidal cycles). Water was sampled at LLW. Mean exchange for neap-tides was $E_{av} = 0.22$.

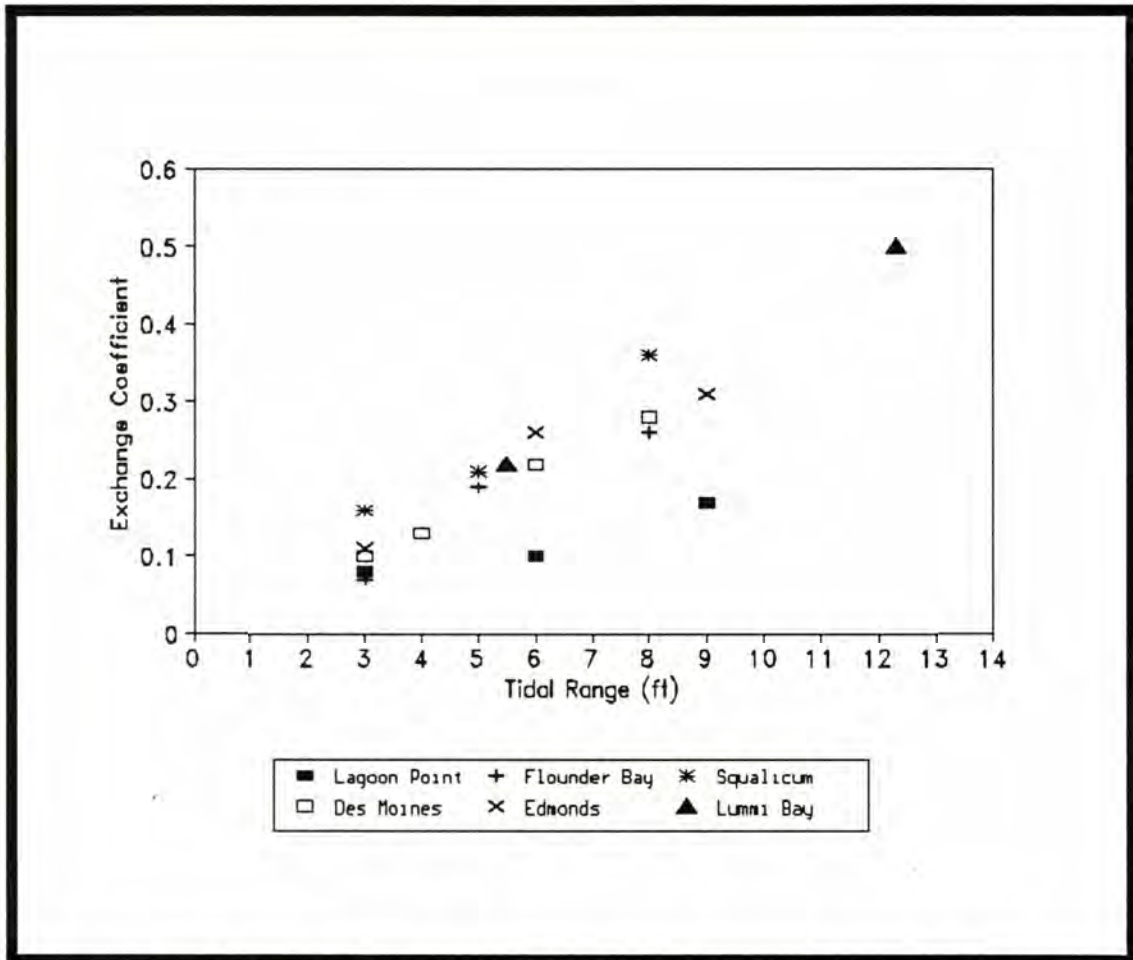


Figure 15. Exchange coefficients vs tidal range for physical-model tests of six Pacific Northwest marinas.

around the model as the tidal current progressed, displacing water already in the model basin. The inflow jet of clear water then began to mix with the dyed water. Enough water was introduced into the model during spring-tide simulations to force the current to circulate water completely around the model.

Water rising over the berm during flooding moved directly outward from the model moorage-basin to cover the berm. The fish pass-throughs in the breakwaters caused two smaller jets of water to form which flowed inward across the berm. The jet on the westerly breakwater forced water

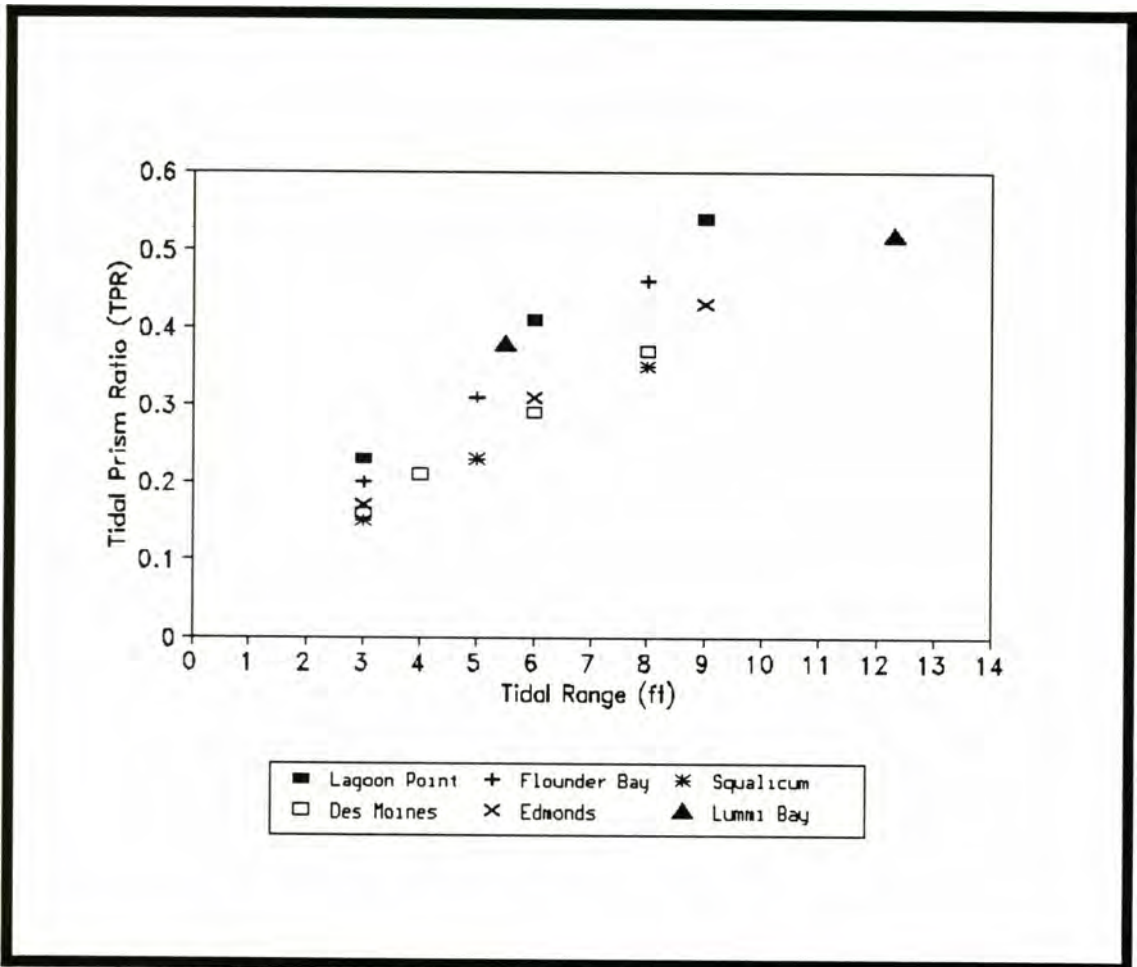


Figure 16. Tidal prism ratios vs tidal range for physical-model tests of six Pacific Northwest marinas.

to move directly across the berm in a similar direction to water in the inflow jet of the entrance channel. Water over the western berm flowed in a similar manner to water in the moorage basin: the dike controlled flow on one side while water moved to the inside unobstructed. Fresh water on the west berm moved about two thirds of the length of the western berm before circulating inward toward the center of the model moorage-basin. Water in the south corner of the model moorage-basin and water over the south corner of the berm was dragged by the in-flowing water and began to form a secondary, clockwise circulation-gyre in the

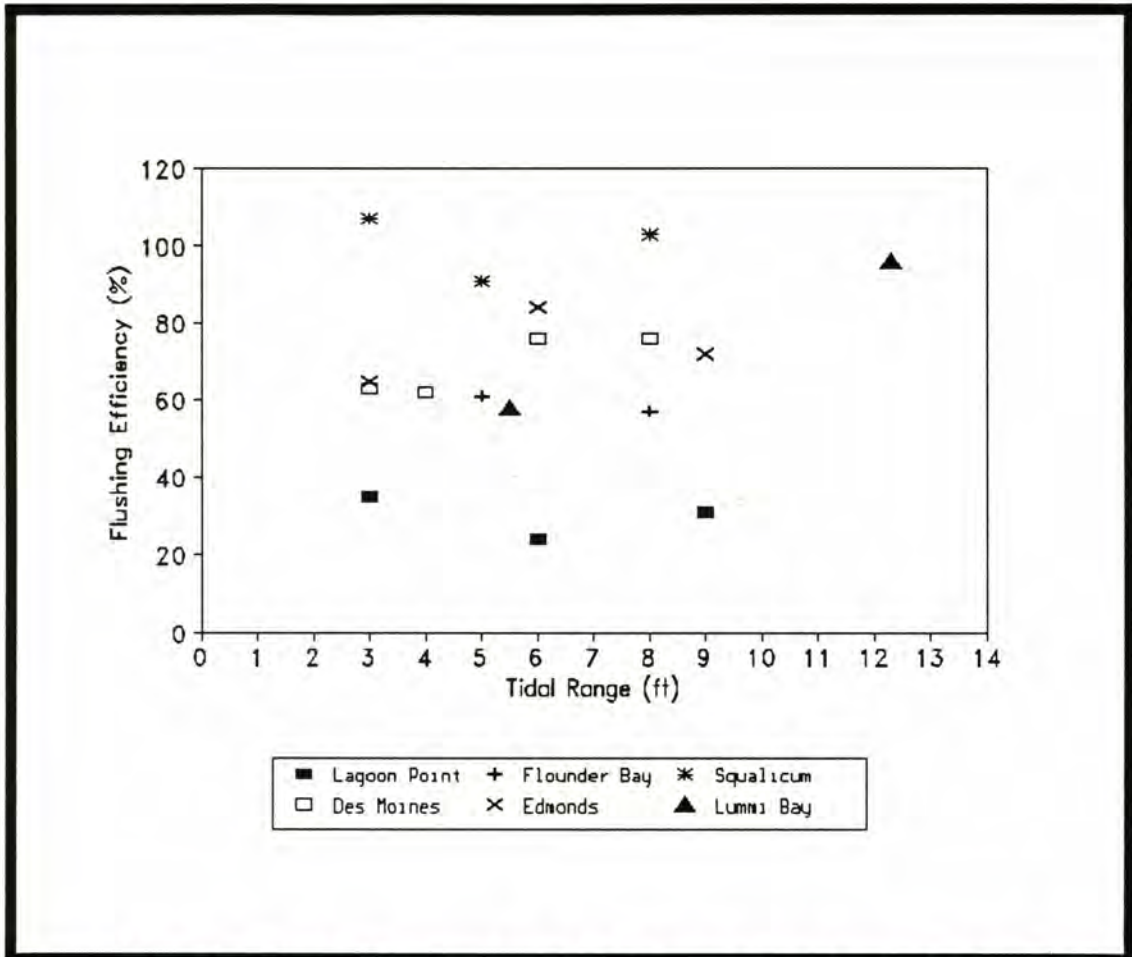


Figure 17. Flushing efficiency vs tidal range for physical-model tests of six Pacific Northwest marinas.

south corner. A similar but less-active clockwise gyre also formed in the north corner. The overall effect was that the model had three circulation-gyres by HHW.

Water began to flow out of the physical model as the tide approached HHW. Dyed water moved outward in small jets through the fish pass-throughs over the berm and was also visible moving outward in the channel. Most water continued to move in the circulation-gyres and remain within the model as the ebb from HHW to HLW began. Momentum of the circulation gyres was lost fairly rapidly as the ebb proceeded. In

contrast to flood conditions, water flowed more linearly toward the model entrance during the ebb. The gyres were distorted as water moved to the channel. Some dyed water moved out of the confines of the channel and onto the model tidal-flat region. By HLW the circulation-gyres had lost most of their energy. Contrasting light and dark streams of water showed the forms of the gyres, but little movement was observed. These forms extended over the areas of both the model moorage-basin and berm at HLW.

The tidal range between HLW and LHW (Table 3) was small enough to prevent a large input of energy to the circulation-gyres created during the LLW-to-HHW flood period. Very little water movement was observed during the smaller flood-tide rise. In the central region of the model a greater water mass allowed continued circulation. The shallow berm area displayed the least amount of movement. Streams of dye formed during the previous larger flood-tide rise continued to stagnate during the smaller flood-tide rise. By the end of the smaller flood, a nearly complete cessation of water motion in the model was observed.

The ebb from LHW to LLW destroyed the circulation-formed patterns of dye and water in the physical model. Water flowed directly toward the entrance as the tide ebbed. Water moved from the berm to the moorage-basin, as the berm was exposed by the falling tide. Local mixing along the inner edges of the berm occurred as the water drained into the moorage-basin from the berm. Water moving through the channel bend outside the marina entrance displayed helical flow.

The tides of the second model test-day produced a similar behavior of tidal currents to those described.

Neap-Tide Trial Runs

The initial conditions for neap-tide trial runs were similar to those of spring-tide simulations. Water currents in the physical model were likewise similar to those observed in spring-tide simulations. An obvious difference from the spring-tide runs was that the smaller tidal-range reduced the energy input to tidal currents in the model. Hence, the ability to circulate water in the model was reduced. The flood tide, from LLW to LHW, forced water into the model as a lobe along the bottom of the channel. The lower velocity created less turbulence than that observed in spring-tide trial runs. The water was less mixed as a result. The entering lobe of water moved into the model, extending furthest along the access channel on the western portion before beginning to mix with the dyed water. The LLW-to-LHW flood tide did not cover the berm, and circulation was restricted to the moorage-basin within the model. At the end of the flood, very little circulation had been observed.

The ebb from LHW to HLW deformed any circulation-gyres which formed as water flowed out of the model. Visible change in bluing concentration in the water was minimal for the first flood and ebb.

The HLW-to-HHW flood induced a stronger current and created a counter-clockwise circulation-gyre in the model, similar to those observed in spring-tide trial runs. The gyre tended to form in the third of the model nearest to the entrance and move toward the rear of the model as it circulated. By the end of the flood, water throughout the model was affected. Secondary clockwise circulation-gyres formed, similar to those in spring-tide trial runs. Water in the south and

north corners was moved by those gyres. A pattern observed for neap-tides which differed from spring-tides was that the reduced energy-input prevented water from being completely circulated during the larger flood-tide rise in neap-tide simulations. The north corner of the model therefore appeared darker at the end of the flood, because the water there had not been mixed and diluted with water of the inflow jet.

The ebb from HHW to HLW slowed the circulation-gyres as the water volume and mass decreased and direction of flow reversed at the model entrance. As with other ebbing, water in the model tended to flow directly toward the entrance.

DISCUSSION

Tidal Exchange

The results shown in Figures 15 through 17 were based on maximum ranges for each tidal simulation. Flushing of the marina model increased with increasing tidal range.

Less apparent from the quantitative data were the observed concentrations of bluing, which were darker in color toward the centers of the main circulation-gyres during and after trial runs. Figure 13 shows a more prominent central area of lower exchange-coefficients in spring-tide trial runs; but the trend is less visible in Figure 14, because weaker circulation did not form prominent gyres like those of the spring runs. During neap-tide trial runs, ebbing water flowed directly toward the entrance and destroyed the circulation-gyres. The energy in the neap gyres was lost during the larger ebb-tide of each trial run.

The south and north corners of the model displayed lower-than-average exchange-coefficients in neap trial runs and higher-than-average exchange-coefficients in spring runs. Neap trial-runs, as a result of smaller volumes and lower velocities, did not force the mixing of water as strongly as did spring runs. The spring trial-runs forced a greater inflow of clear water around the edges of the model, which subsequently flowed into the model moorage-basin from the berm as the tide dropped below the level of the berm. Less water volume over the berm and reduced mixing during neap trial-runs account for the different behavior between the simulations. In both simulations, exchange-coefficients at the sample position nearest the entrance were less than the mean value.

This fact can be explained by the large volumes of mixed water and bluing which ebbed toward the entrance. The mixture in both cases was observed to be related to the central portion of the circulation-gyre as the gyre was distorted toward the entrance. Water in the center tended to move toward the entrance more quickly than did water around the edges, which was susceptible to more friction as it moved across the surface of the model.

As stated above, during trial-runs it was observed that the centers of the circulation-gyres were darker than the water moving around them. In secondary circulation-gyres no problem was perceived in overall water quality as those gyres were destroyed each time the tidal level passed below the level of the berm.

Effects of the Berm on Circulation

The modeled berm had several effects on circulation. Water moving outward onto the berm flooded in the direction of least elevation. Generally, the berm first flooded at the end of the model most distant from the entrance, with the water then moving across the berm toward the entrance, until it was met by water flowing over the berm from the fish pass-throughs. This phenomenon enhanced circulation within the secondary gyre in the south corner, and had a similar but less-pronounced effect on the secondary gyre in the north corner.

A second phenomenon relating to the berm was the rapid loss of energy in water over the berm. The shallowness of water on the berm increased the effect of boundary friction in the water. Consequently, during the smaller tides in each trial run, inertial forces prevailed.

Streams of water containing varied amounts of dye were observed to have little or no motion during the smaller ebb and flood tides of each trial-run. The variably-colored water, observed as streams, experienced minimal mixing from the berm. Stagnant conditions remained until the larger ebb-tide fall forced water back into the marina basin and channel where it was either mixed with new water or flushed out of the model.

Larger ebb-tides had the effect of lowering the water level below the berm. Water over the berm flowed directly toward the moorage-basin as the water level fell. Some water flowed with enough energy to create minor turbulence at the inner edge of the berm. Some mixing of water was observed as a light-colored band parallel to the berm edge. The light-colored band was clearer water which was introduced during the previous flood and had moved to the outer edges of the berm as it circulated. That water remained over the berm during smaller ebb and flood tides, until it drained back into the model moorage-basin during the larger ebb-tides of each trial-run.

Effects of Sloping Dikes and Berm-Walls on Circulation

The major impact that the dikes and berm-walls exerted was as physical barriers which helped to direct water currents within the model. Water flowing in through the entrance was confined by a berm-wall on one side but could flow counter-clockwise toward the center of the model to form the circulation-gyres. The effect did not differ drastically from those observed in previous marina circulation studies (eg., Nece et al., 1980). Because this study was done using a fixed-bed model, the possibility of erosion of the berm and slope was not

addressed. The sloped dikes and berm-walls did not appear to have a substantially different effect on circulation within the model from the vertical walls of previous models (eg., Nece et al., 1979; Nece et al., 1980).

Effects of Non-uniform Bottom Depth

Non-uniform bottom depth may have enhanced vertical-mixing of water in the model. In most trial runs, water initially entered the model along the bottom of the channel. Those lobes of incoming water were forced along the bottom of the model moorage-basin as the flood-tide progressed. This phenomenon was similar to one observed by Richey and Smith (1977) in a prototype marina. The end of the basin located furthest from the entrance, with its shallower depths, helped to induce mixing by forcing incoming bottom water upward into the overlying water. The access-channel also helped direct water to the south corner of the model and stimulate formation of circulation-gyres.

In the north corner of the basin, water appeared to be darker and less mixed. Values for exchange coefficients suggest that the greater depth was responsible for greater apparent coloration of water, although water in that portion of the basin was least affected by the inflow jets of new water flowing into the model and therefore may be less mixed.

Effect of a Simulated Diurnal Inequality

The Lummi Bay model was different from previous models in that it incorporated a simulated diurnal inequality. The overall effect of the diurnal inequality on gross exchange-coefficients does not appear to

have been major, as Figures 15 through 17 show. Another observed effect, however, was that water tended to stagnate during the smaller ebb and flood tides of each trial run, but was flushed out as larger ebb-tides fell. This phenomenon does not occur in models based on repetitive and sinusoidal tides to the degree observed in these model tests. It is stressed here that water quality in the proposed marina will vary with the volume of water involved in a tidal exchange. The standards for water quality set by the Washington State Department of Fisheries (U.S. Army Corps of Engineers, 1988), which were mentioned in the Statement of Problem above, were exceeded in spring-tide simulations but were not met by neap-tide simulations.

The flushing-efficiency, predicted to be about 100%, also varied as a result of tidal range. Water quality in the model was dependent on the amount of water exchanged. The realistic smaller ranges, experienced as a result of the diurnal inequality, may therefore reduce water quality on a daily basis.

CONCLUSIONS

The conclusions reached in this physical-model investigation of the tidal-flushing potential in the proposed Lummi Bay Marina are as follows.

This study suggests a tendency for a decreased water quality during times of smaller tides, but a broader range of data is needed to fully understand the entire tidal system in Lummi Bay. A variety of factors relating to water quality and tidal-flushing were not considered in this study. Sedimentation, boats, slips, wind, temperature, water stratification, freshwater runoff, and the interactions between those factors, would have an impact on water quality in the proposed marina.

Exchange coefficients in the physical model increased with increasing tidal range. Overall, exchange was best during spring-tide simulations, but water tended to stagnate during the small ebb and flood cycles of both spring and neap simulations. Water quality in the proposed Lummi Bay Marina will probably also vary with tidal range. Water in the marina may be vulnerable to depletion of dissolved oxygen and to increased temperatures during periods of smaller tidal exchange.

Circulation gyres forming in the marina contain less mixed water toward their centers. The primary counterclockwise-gyre should retain enough momentum to be somewhat intact at LLW, although neap tides would not induce as strong a circulation of water as would spring tides. Secondary clockwise-gyres may form in the north and south corners of the marina over the berm. Reduced water quality might be a result, but

those gyres would be destroyed each time the berm is exposed, so that the secondary gyres would likely cause short-term problems only.

The physical model and tide-generator provided a means for studying tidal-flushing at Lummi Bay. The tide-generator was used to provide two tidal-ranges representative of regional spring and neap tides. Construction of both the physical model and tide-generator demonstrate that for relatively simple problems relating to tidal systems this method can be applied in lieu of a large-scale laboratory apparatus.

Spectrophotometry can be used on a variety of tracers provided that they absorb distinguishable wavelengths of light. An added advantage for future studies is that spectrophotometers are relatively inexpensive and common, and they produce accurate, precise data.

Finally, it is emphasized that this was a predictive study. The data that were collected allowed for some comparisons to be made between model and prototype. In the event of construction of the Lummi Bay Marina, the problem of tidal-flushing should be further studied using a field approach to verify the results of this study and to insure adequate water quality in the proposed marina.

REFERENCES CITED

- Bird, E. C. F., 1984, Coasts: An introduction to coastal geomorphology, third edition: New York, Basil Blackwell, Inc., 320 p.
- Bortelson, G. C., Chrzastowski, M. J., and Helgerson, A. K., 1980, Historical changes of shoreline and wetland at eleven major deltas in the Puget Sound region, Washington: U.S. Geological Survey Hydrological Investigations Atlas, HA-617, 11 plates.
- Christian, G. D., 1977, Analytical chemistry, second edition: New York, John Wiley and Sons, 648 p.
- Easterbrook, D. J., 1973, Environmental geology of western Whatcom County, Washington: in-house report, Western Washington State College, Bellingham, Wa., 78 p., 7 plates.
- Falconer, R., 1980, Water quality simulation study of a natural harbor: Journal of Waterway, Port, Coastal, and Ocean Engineering, ASCE, v. 112(1), p. 15-33.
- Harris, D. L., 1981, Tides and tidal datums in the United States: Special Report no. 7, U.S. Army Corps of Engineers, Coastal Engineering Research Center, Ft. Belvoir, Va., 382 p.
- Hudson, R. Y., Herrman, F. A., Jr., Sager, R. A., Whalin, R. W., Keulegan, G. H., Chatham, C. E., Jr., and Hales, L. Z., 1979, Coastal hydraulic models: Special Report no. 5, U.S. Army Corps of Engineers, Coastal Engineering Research Center, Ft. Belvoir, Va., 531 p.
- Jacobsen, E. E., 1980, Net shore-drift of Whatcom County, Washington: Master of Science Thesis, Western Washington University, Bellingham, Wa., 79 p.
- Mofjeld, H. O., and Larsen, L. H., 1984, Tides and tidal currents of the inland waters of Western Washington: NOAA Technical Memorandum ERLPEML-56, United States Dept. of Commerce, Pacific Marine Environmental Laboratory, Seattle, Wa., 52 p.
- Nece, R. E., 1984, Planform effects on tidal flushing of marinas: Journal of Waterway, Port, Coastal, and Ocean Engineering, ASCE, v. 110(2), p. 251-269.
- Nece, R. E., and Forsyth, G. W., 1980, Annotated bibliography on tidal flushing and circulation in marinas: Technical Report no. 67, Charles W. Harris Hydraulics Laboratory, University of Washington, Seattle, 71 p.
- Nece, R. E., Richey, E. P., and Rhee, J., 1979, Effects of planform geometry on tidal flushing and mixing in marinas: Technical

- Report no. 62, Charles W. Harris Hydraulics Laboratory, University of Washington, Seattle, 74 p.
- Nece, R. E., Smith, H. N., and Richey, E. P., 1980, Tidal calculations and flushing in five western Washington marinas: Technical Report no. 63, Charles W. Harris Hydraulics Laboratory, University of Washington, Seattle, 50 p.
- Nece, R. E., Welch, E. B., and Read, J. R., 1975, Flushing criteria for salt water marinas: Technical Report no. 42, Charles W. Harris Hydraulics Laboratory, University of Washington, Seattle, 50 p.
- Richey, E. P., and Nece, R. E., 1972, Lake Crockett small boat basin circulation study: Technical Report no. 33, Charles W. Harris Hydraulics Laboratory, University of Washington, Seattle, 24 p.
- Richey, E. P., and Smith, N. H., 1977, Birch Bay Marina: Hydraulics of proposed expansion: Technical Report no. 53, Charles W. Harris Hydraulics Laboratory, University of Washington, Seattle, 38 p.
- Slotta, L. S., and Noble, S. M., 1977, Use of benthic sediments as indicators of marina flushing: Sea Grant Publication no. ORESU-T-77-007, Oregon State University, Corvallis, 56 p.
- Smelser, C. R., 1970, Sequent occupance of the Nooksack River Valley and the influence of man on the rate of sediment delivery to Bellingham Bay: Master of Science Thesis, Western Washington State College, Bellingham, Wa., 107 p.
- Sokal, R. R., and Rohlf, F. J., 1981, Biometry: the principles and practice of statistics in biological research, second edition: New York, W. H. Freeman and Co., 859 p.
- Thabet, R. A. H., Verboom, G. K., and Akkerman, G. J., 1985, Two dimensional modelling of tidal motion for harbour studies: Publication no. 344, Delft Hydraulics Laboratory, Delft, The Netherlands, p. 23-32.
- U.S. Army Corps of Engineers, 1988, Final definite project report and definite environmental impact statement, Lummi Bay Marina, Whatcom County, Washington: Department of the Army, Seattle District, Corps of Engineers, Seattle, 443 p.
- U.S. Department of Commerce, 1988, High and low water predictions, west coast of North and South America, including the Hawaiian Islands (issued 1987): U.S. Dept. of Commerce, NOAA-NOS, U.S. Government Printing Office, Rockville, Md., 234 p.
- Ward, P. R. B., 1973, Measurement of dye concentrations by photography: Journal of the Environmental Engineering Division, ASCE, v. 99:EE3, p. 165-175.